



Research article

[urn:lsid:zoobank.org:pub:738E2549-40F3-48E5-9123-F4F2B0D2B834](https://zoobank.org/pub:738E2549-40F3-48E5-9123-F4F2B0D2B834)

Two new species of *Scolopocryptops* centipedes from southern Japan (Chilopoda: Scolopendromorpha: Scolopocryptopidae)

Taro JONISHI ^{1,*} & Takafumi NAKANO ²

^{1,2}Department of Zoology, Graduate School of Science, Kyoto University, Kyoto 606-8502, Japan.

*Corresponding author: ykn347635@gmail.com

²Email: nakano@zoo.zool.kyoto-u.ac.jp

¹[urn:lsid:zoobank.org:author:003B527C-D6A1-4BBE-9B3E-7779713530CF](https://zoobank.org/author:003B527C-D6A1-4BBE-9B3E-7779713530CF)

²[urn:lsid:zoobank.org:author:FE6B9521-5C9E-43C5-B492-08B0D0590E1B](https://zoobank.org/author:FE6B9521-5C9E-43C5-B492-08B0D0590E1B)

Abstract. The blind centipede genus *Scolopocryptops* Newport, 1844 comprises two lineages: the “Asian/North American” group and the “Neotropical/Afrotropical” group. The former can be further split into two groups, a clade comprising *Scolopocryptops elegans* (Takakuwa, 1937) and *Scolopocryptops curtus* (Takakuwa, 1939), and a clade comprising all other “Asian/North American” species. Here, *Scolopocryptops miyosii* sp. nov. from Kyushu and Amami Island and *Scolopocryptops brevisulcatus* sp. nov. from Izena Island and Okinawa Island in southern Japan are described. The two new species have external features similar to *S. elegans* and *S. curtus*. They can be distinguished from most other “Asian/North American” *Scolopocryptops* by the absence of complete sulcus/sulci along the lateral margin of the cephalic plate and the presence of sternal longitudinal sulci. They can be distinguished from each other by several external features, such as the density of antennal setae and the shape of the anterior margin of the coxosternite. Phylogenetic analyses using nuclear and mitochondrial markers also support the monophyly of the four species, which form a clade sister to all other “Asian/North American” *Scolopocryptops*.

Keywords. Allopatric distribution, Asian/North American group, Japanese Archipelago, Ryukyu Islands, species delimitation.

Jonishi T. & Nakano T. 2023. Two new species of *Scolopocryptops* centipedes from southern Japan (Chilopoda: Scolopendromorpha: Scolopocryptopidae). *European Journal of Taxonomy* 908: 155–182.
<https://doi.org/10.5852/ejt.2023.908.2345>

Introduction

Centipedes of the genus *Scolopocryptops* Newport, 1844 are blind species that mostly inhabit the forest litter layer. *Scolopocryptops* currently consists of 31 species and subspecies distributed in southern Canada, USA, Mexico, Central America, the Antilles, South America, West Africa, China, Japan, Korea, Taiwan, and Vietnam; they have also been documented in India, the Philippines, Indonesia, New Guinea and Fiji (Chagas-Jr. *et al.* 2023; Le *et al.* 2023). The genus comprises two distinct lineages: the “Asian/North American” group and the “Neotropical/Afrotropical” group (Chagas-Jr. 2008; Edgecombe *et al.*

2012; Vahtera *et al.* 2013). Both morphological and molecular data suggest that the Asian/North American *Scolopocryptops* can be further divided into two groups: a clade comprising *S. elegans* (Takakuwa, 1937) and *S. curtus* (Takakuwa, 1939), which is endemic to Far East Asia, and a clade consisting of the rest of the Asian/North American species (Jonishi & Nakano 2022). *Scolopocryptops elegans* and *S. curtus* share two characters that distinguish them from most other Asian/North American species, i.e., the absence of complete sulcus/sulci along the lateral margin of the cephalic plate and the presence of sternal longitudinal sulci (Takakuwa 1937, 1939, 1940; Chao & Chang 2008; Jonishi & Nakano 2022). Other features shared by these two species include their large body size, reddish body color, and the lack of a transparent margin on the dorsal brush of article 3 of the second maxilla (Jonishi & Nakano 2022).

Scolopocryptops elegans, described from Shikoku, Japan, has been widely documented in the Japanese Archipelago, Izu Islands, and the Ryukyu Islands (Takakuwa 1937; Shinohara 1949; Takashima 1949; Ikehara & Shimojana 1971; Takano 1979; Ômine 1987). *Scolopocryptops curtus* was described from southern Taiwan and has been recorded in southern Kyushu, the Ryukyu Islands, and Taiwan (Takakuwa 1939; Miyosi 1961; Ômine 1969, 2002; Ômine & Ito 1998; Chao & Chang 2003, 2008; Jonishi & Nakano 2022). These records indicate that *S. elegans* and *S. curtus* are sympatrically distributed in Kyushu and the Ryukyus. However, because many of these studies did not clarify the taxonomic accounts of specimens in detail, there is reason to question their identification as *S. elegans* and *S. curtus* and thus the distribution of these two species in southern Japan. Although specimens from Iriomote Island in the southernmost Ryukyu Islands were clearly identified as *S. curtus* on the basis of both morphological and molecular data (Jonishi & Nakano 2022), the systematic status of “*S. elegans*/*S. curtus*-like” specimens from other Ryukyuan islands and Kyushu requires clarification.

Several unidentified specimens of *Scolopocryptops* were recently obtained from Kyushu and the Ryukyu Islands. All these specimens have external features similar to *S. elegans* and *S. curtus*, but they differ in several characters, such as the density of antennal setae, the presence/absence of the cephalic marginal sulcus, and the shape of the anterior margin of the forcipular coxosternite. Here, we describe them as two new species. The phylogenetic positions of the two new species, including their relationships with *S. elegans* and *S. curtus*, were estimated using nuclear and mitochondrial DNA sequences.

Material and methods

Taxon sampling and morphological examination

A total of 21 unidentified specimens of *Scolopocryptops* were collected from Oita and Kagoshima Prefectures in Kyushu, and Amami, Izena, and Okinawa Islands in the Ryukyu Islands. Additionally, a specimen of *S. elegans* was collected from Tokyo, eastern Honshu (35.737° N, 139.237° E) on 12 April 2022 (Fig. 1); a specimen of *S. ogawai* Shinohara, 1984 from its type locality (Shizuoka; 34.740° N, 137.978° E; 22 March 2021; KUZ Z4395) was also included in molecular analyses. Specimens were fixed in 80% or 99% ethanol after they had been placed in 30% ethanol for a while, and then preserved in 80% ethanol. Leg-bearing segment 23 of several specimens were dissected to examine genital morphology. All the specimens were examined using a Leica M125C stereoscopic microscope with a drawing tube (Leica Microsystems, Wetzlar, Germany). The specimens were photographed using a Sony a6500 digital camera and a 65 mm macro lens, and a Leica MC170 HD digital camera on the Leica M125C. Images captured with the Leica MC170 were processed using the software Leica Application Suite ver. 4.1.2. Specimens examined are deposited in the Zoological Collection of Kyoto University.

The terminology for external morphology follows Lewis *et al.* (2005) and Bonato *et al.* (2010). Growth stadium (juvenile, subadult, or adult) was determined based on the body length (Schileyko 2014, 2018) and development of genital segments (Jonishi & Nakano 2022). For dissected adults and individuals with everted genital organs, sex was determined following Takakuwa (1933); the terminology for genital organs follows Demange & Richard (1969) and Iorio (2003).

Institutional abbreviations

AMNH = American Museum of Natural History, New York, USA
 MCZ = Museum of Comparative Zoology, Harvard University, Cambridge, USA
 SYSU = National Sun Yat-sen University, Kaohsiung, Taiwan
 KUZ = Zoological Collection of Kyoto University, Kyoto, Japan

DNA extraction, PCR, and DNA sequencing

Total DNA was extracted from leg samples using a DNA Blood and Tissue Kit (Qiagen, Hilden, Germany) or a NucleoSpin Tissue kit (Macherey-Nagel, Duren, Germany). Phylogenetic analyses were conducted using nuclear internal transcribed spacer 2 (ITS2), 28S rRNA (28S), and mitochondrial cytochrome *c* oxidase subunit 1 (COI) markers following previous studies (e.g., Edgecombe *et al.* 2012, 2019). The primer pairs used are as follows: the 5.8SF/28SRev (Murienne *et al.* 2011) for ITS2, 28Sa/28Sb (Whiting *et al.* 1997) for 28S, and LCO1490/HCO2198 (Folmer *et al.* 1994) or the reverse primer HCOoutout (Schwendinger & Giribet 2005) for COI, respectively. Each PCR was performed using TaKaRa Ex Taq DNA polymerase or TaKaRa Ex Premier DNA Polymerase (Takara Bio Inc., Shiga, Japan). For

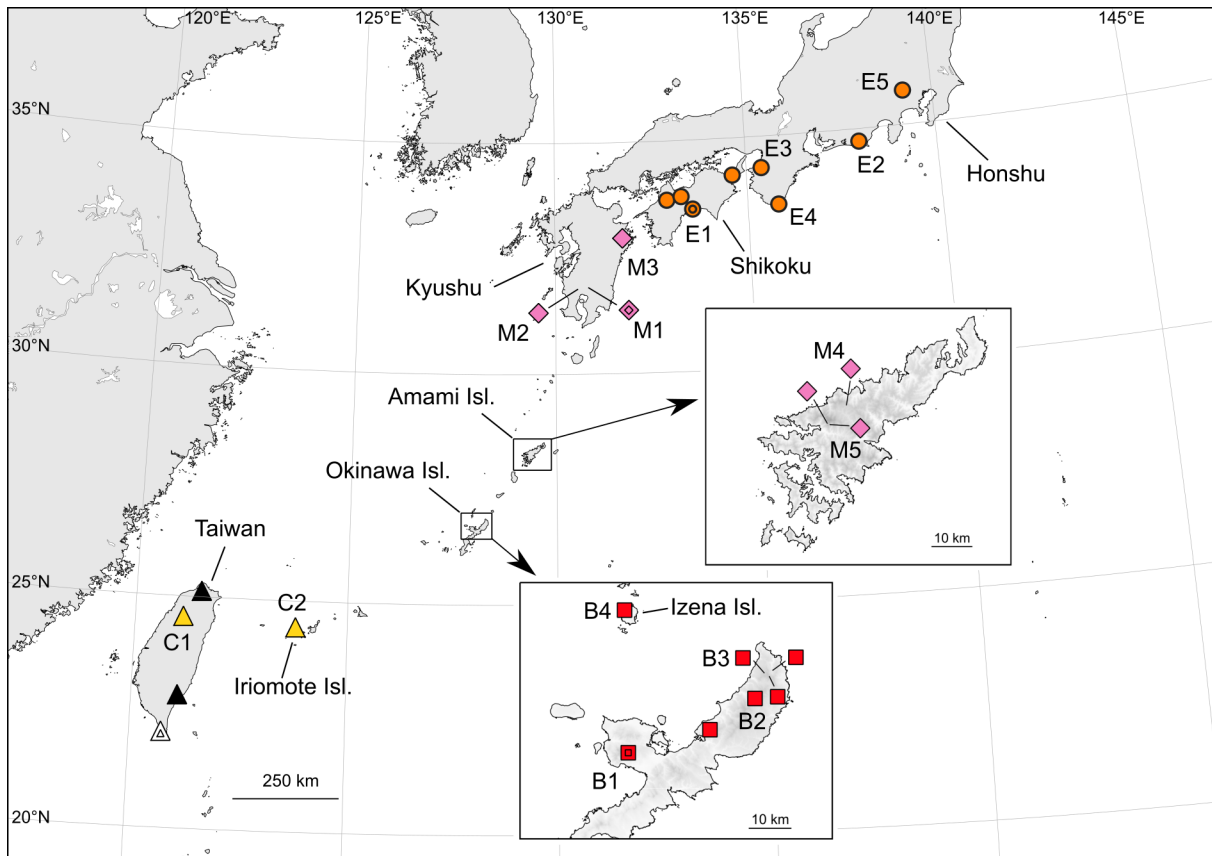


Fig. 1. Map showing the collection localities of *Scolopocryptops elegans* (Takakuwa, 1937), *S. miyosii* sp. nov., *S. brevisulcatus* sp. nov., and *S. curtus* (Takakuwa, 1939) in the present study and Jonishi & Nakano (2022). Orange circles: *S. elegans*; pink diamonds: *S. miyosii* sp. nov.; red squares: *S. brevisulcatus* sp. nov.; yellow triangles: *S. curtus*; black triangles: localities of the sequence data of *S. curtus* obtained from INSD (see Table 1). Shapes with two lines indicate the type localities of each species (*S. curtus* from its type locality was not examined). Locality numbers (E1–E5, M1–M5, B1–B4, C1 and C2) are shown in Fig. 2 and Table 1.

ITS2, 28S and COI, reactions were performed using a LifeECO Thermal Cycler (Bioer Technology, Hangzhou, China), a GeneAmp PCR System 9700 (Thermo Fisher Scientific, Waltham, USA), and a T-100 Thermal Cycler (Bio-Rad, Hercules, USA), respectively. The PCR mixtures were heated to 94°C for 5 min, followed by 35 cycles at 94°C (10 s), 50–60°C for ITS2, 60°C 28S, or 50°C for COI (20 s), and then 72°C (48 s for ITS2, 30 s for 28S, and 42–48 s for COI), with a final extension at 72°C for 6 min. The cycle sequencing reactions were conducted using a SupreDye Cycle Sequencing Kit (M&S Techno Systems, Osaka, Japan). Each cycle sequencing mixture was heated to 96°C (2 min), followed by 40 cycles of 96°C (10 s), 50°C (5 s), and then 60°C (48 s). The cycle-sequencing products were collected by ethanol precipitation and sequenced on an ABI 3130xl Genetic Analyzer (Thermo Fisher Scientific). Chromatograms were visualized and assembled using the software DNA BASER (Heracle Biosoft S.R.L., Argeş, Romania). In total, 37 sequences were newly obtained, and deposited in the International Nucleotide Sequence Databases (INSD) through the DNA Data Bank of Japan (Table 1).

Molecular analyses

In addition to the newly obtained 37 sequences, 18 sequences of six Japanese and Taiwanese species of *Scolopocryptops* (see Jonishi & Nakano 2022) were included in the present dataset (Table 1). Also, a total of 13 sequences of Scolopocryptopidae Pocock, 1896 were obtained from INSD (Table 1) from five of the “Asian/North American” nominal species, viz., *S. curtus*, *S. nigridius* McNeil, 1887, “*S. nipponicus*” Shinohara, 1990 sensu Edgecombe *et al.* (2012) (= *S. spinicaudus* Wood, 1862; see Shelley 2002), *S. sexspinosus* (Say, 1821), and *S. spinicaudus*, and the “Neotropical/Afrotropical” nominal species “*S. mexicanus*” Humbert & Saussure, 1869 sensu Edgecombe *et al.* (2012) (= *S. ferrugineus* (Linnaeus, 1767); see Attems 1930); *Newportia monticola* Pocock, 1890 was utilized as an outgroup taxon. Based on the results of the preliminary phylogenetic analyses, a 28S sequence of “*S. mexicanus*” (JX422593) was excluded from the dataset to prevent long branch attractions.

The nuclear ITS2 sequences were aligned using MAFFT L-INS-i (Kato & Standley 2013), and the 28S sequences were aligned by MAFFT Q-INS-i (Kuraku *et al.* 2013; Kato *et al.* 2019), considering the RNA secondary structure information; non-conserved regions of both genes were trimmed using Gblocks (Castresana 2000). Alignment of the mitochondrial COI was trivial because no indels were observed. The aligned sequences of ITS2, 28S, and COI were 849, 505, and 658 bp, respectively. The first four positions of COI were missing in most of the sequences, and this portion of COI was excluded from the analyses. Thus, the concatenated sequence yielded 2008 bp of aligned positions.

Phylogenetic trees were reconstructed by maximum likelihood (ML) and Bayesian Inference (BI). The best-fit partition scheme and models were identified based on the Bayesian information criterion (BIC) using PartitionFinder ver. 2.1.1 (Lanfear *et al.* 2016) with the ‘all’ algorithm. The selected partition schemes were as follows: TRNEF+I or SYM+I for COI 1st position, F81+I for COI 2nd position, TIM+G or HKY+G for COI 3rd position, TRNEF+G or GTR+G for 28S, and TVMEF+G or SYM+G for ITS2. The ML phylogenetic tree was reconstructed using IQ-TREE ver. 1.6.12 (Nguyen *et al.* 2015) with ultrafast bootstrapping (UFBoot; Hoang *et al.* 2017) conducted with 1000 replicates. The BI tree and Bayesian posterior probabilities (BPP) were estimated using MrBayes ver. 3.2.7 (Ronquist *et al.* 2012). Two independent runs of four Markov chains were conducted for 10 million generations, and the tree was sampled every 100 generations. According to parameter estimates and assessment of convergence using Tracer ver. 1.7.2 (Rambaut *et al.* 2018), the first 25 000 trees were discarded. Uncorrected pairwise distances for COI sequences (633–654 bp) were calculated with MEGA X (Kumar *et al.* 2018), with pairwise deletion of missing data.

Species delimitation tests were used to infer putative species boundaries. As the phylogenetic analyses failed to reconstruct robust phylogeny of the “*S. elegans/S. curtus*-like” specimens, the following non-tree-based approaches were only applied to the partial COI sequences: Automatic Barcoding Gap

Table 1 (continued on next page). Samples used for the molecular analyses. The information on the voucher is accompanied by the collection locality and the INSD accession numbers of the DNA sequences. Locality numbers are shown in Figs 1–2.

Species	Voucher #	Locality	Locality #	ITS2	INSD # 28S	COI	References
<i>Scolopocryptops</i>							
<i>S. elegans</i>	KUZ Z4062	Katsurahama, Kochi, Japan	E1	LC741566	LC700494	LC700493	This study for ITS2; Jonishi & Nakano (2022) for 28S and COI
<i>S. elegans</i>	KUZ Z4068	Fukuroi, Shizuoka, Japan	E2	LC741567	LC700496	LC700495	This study for ITS2; Jonishi & Nakano (2022) for 28S and COI
<i>S. elegans</i>	KUZ Z4071	Kinokawa, Wakayama, Japan	E3	LC741568	LC700498	LC700497	This study for ITS2; Jonishi & Nakano (2022) for 28S and COI
<i>S. elegans</i>	KUZ Z4073	Higashimuro, Wakayama, Japan	E4	LC741569	LC700500	LC700499	This study for ITS2; Jonishi & Nakano (2022) for 28S and COI
<i>S. elegans</i>	KUZ Z4373	Akiruno, Tokyo, Japan	E5	LC741570	LC741571	LC741572	This study
<i>S. miyosii</i> sp. nov.	KUZ Z4375	Kirishima, Kagoshima, Japan	M1	LC741573	LC741574	LC741575	This study
<i>S. miyosii</i> sp. nov.	KUZ Z4377	Aira, Kagoshima, Japan	M2	—	LC741576	LC741577	This study
<i>S. miyosii</i> sp. nov.	KUZ Z4374	Saeki, Oita, Japan	M3	LC741578	LC741579	LC741580	This study
<i>S. miyosii</i> sp. nov.	KUZ Z4380	Yamato, Amami Island, Japan	M4	LC741581	LC741582	LC741583	This study
<i>S. miyosii</i> sp. nov.	KUZ Z4378	Yuwán, Amami Island, Japan	M5	LC741584	LC741585	LC741586	This study
<i>S. brevisulcatus</i> sp. nov.	KUZ Z4389	Mt. Katsuu-dake, Okinawa Island, Japan	B1	—	LC741587	LC741588	This study
<i>S. brevisulcatus</i> sp. nov.	KUZ Z4392	Mt. Fuenchiji, Okinawa Island, Japan	B2	LC741589	LC741590	LC741591	This study
<i>S. brevisulcatus</i> sp. nov.	KUZ Z4386	near Mt. Nishime-dake, Okinawa Island, Japan	B3	LC741592	LC741593	LC741594	This study
<i>S. brevisulcatus</i> sp. nov.	KUZ Z4394	Izena Island, Japan	B4	—	LC741595	LC741596	This study
<i>S. curtus</i>	KUZ Z4079	Tai'an, Miaoli, Taiwan	C1	LC741597	LC700502	LC700501	This study for ITS2; Jonishi & Nakano (2022) for 28S and COI

Table 1 (continued). Samples used for the molecular analyses. The information on the voucher is accompanied by the collection locality and the INSD accession numbers of the DNA sequences. Locality numbers are shown in Figs 1–2.

Species	Voucher #	Locality	Locality #	ITS2	INSD # 28S	COI	References
<i>S. curtus</i>	KUZ Z4081	Iriomote Island, Okinawa, Japan	C2	LC741598	LC700504	LC700503	This study for ITS2; Jonishi & Nakano (2022) for 28S and COI
<i>S. curtus</i>	SYSU Chilo-025	Beitou, Taipei, Taiwan	—	—	—	AB617531	Chao <i>et al.</i> (unpublished)
<i>S. curtus</i>	SYSU Chilo-045	Yanping, Taitung, Taiwan	—	—	—	AB617532	Chao <i>et al.</i> (unpublished)
<i>S. musashiensis</i>	KUZ Z4085	Ichikawa, Chiba, Japan	—	—	LC700512	LC700511	Jonishi & Nakano (2022)
<i>S. nigradius</i>	MCZ DNA100807	North Carolina, USA	—	—	HM453278	AY288744	Vahtera <i>et al.</i> (2012) for 28S; Edgecombe & Giribet (2004) for COI
“ <i>S. nipponicus</i> ”	MCZ IZ-130804	Nagoya, Aichi, Japan	—	—	JX422595	JX422681	Edgecombe <i>et al.</i> (2012)
<i>S. ogawai</i>	KUZ Z4395	Fukuroi, Shizuoka, Japan	—	LC741599	LC741600	LC741601	This study
<i>S. quadristriatus</i>	KUZ Z4083	Uratakao-cho, Hachioji, Tokyo, Japan	—	—	LC700508	LC700507	Jonishi & Nakano (2022)
<i>S. rubiginosus</i>	KUZ Z4082	Enoshima, Kanagawa, Japan	—	LC741602	LC700506	LC700505	This study for ITS2; Jonishi & Nakano (2022) for 28S and COI
<i>S. sexspinosus</i>	MCZ IZ-131450	North Carolina, USA	—	—	AY288710	AY288745	Edgecombe & Giribet (2004)
<i>S. spinicaudus</i>	AMNH IZC-00146514	California, USA	—	—	JX422596	JX422683	Edgecombe <i>et al.</i> (2012)
“ <i>S. mexicanus</i> ”	MCZ IZ-130812	Napo, Ecuador	—	—	—	JX422679	Edgecombe <i>et al.</i> (2012)
Outgroup							
<i>Newportia monticola</i>	MCZ IZ-130777	Parque de Cahuita, Costa Rica	—	—	KF676360	KF676507	Vahtera <i>et al.</i> (2013)

Discovery (ABGD; Puillandre *et al.* 2011) and Assemble Species by Automatic Partitioning (ASAP; Puillandre *et al.* 2021). Partly following Peretti *et al.* (2022), the ABGD analysis was run in a web-based interface (<https://bioinfo.mnhn.fr/abi/public/abgd/abgdweb.html>) using uncorrected pairwise distances, with 1000 steps in a range of prior values of maximum intraspecific distance (P) of 0.001–0.15, with no prior minimum relative gap width (X) specified. The ASAP analysis was performed using a webserver (<https://bioinfo.mnhn.fr/abi/public/asap/asapweb.html>) using uncorrected pairwise distances with the default parameters.

Results

Molecular phylogeny and species delimitation

The topologies of the ML ($\ln L = -9372.51$; not shown) and BI (mean $\ln L = -9352.57$; Fig. 2) trees were nearly identical. Within the “Asian/North American” group (UFBoot = 91%, BPP = 0.99), *S. elegans*, *S. curtus*, *S. miyosii* sp. nov., and *S. brevisulcatus* sp. nov. comprised a monophyletic clade (UFBoot = 98%, BPP = 1.0) sister to all other species. *Scolopocryptops elegans* (UFBoot = 97%, BPP = 1.0) was resolved as a sister group of the other three species, which formed a clade, although the monophyly of this group was supported only in BI analysis (UFBoot = 80%, BPP = 0.97). Within this clade, *S. brevisulcatus* received full support (UFBoot = 100%, BPP = 1.0), and *S. curtus* was also recovered

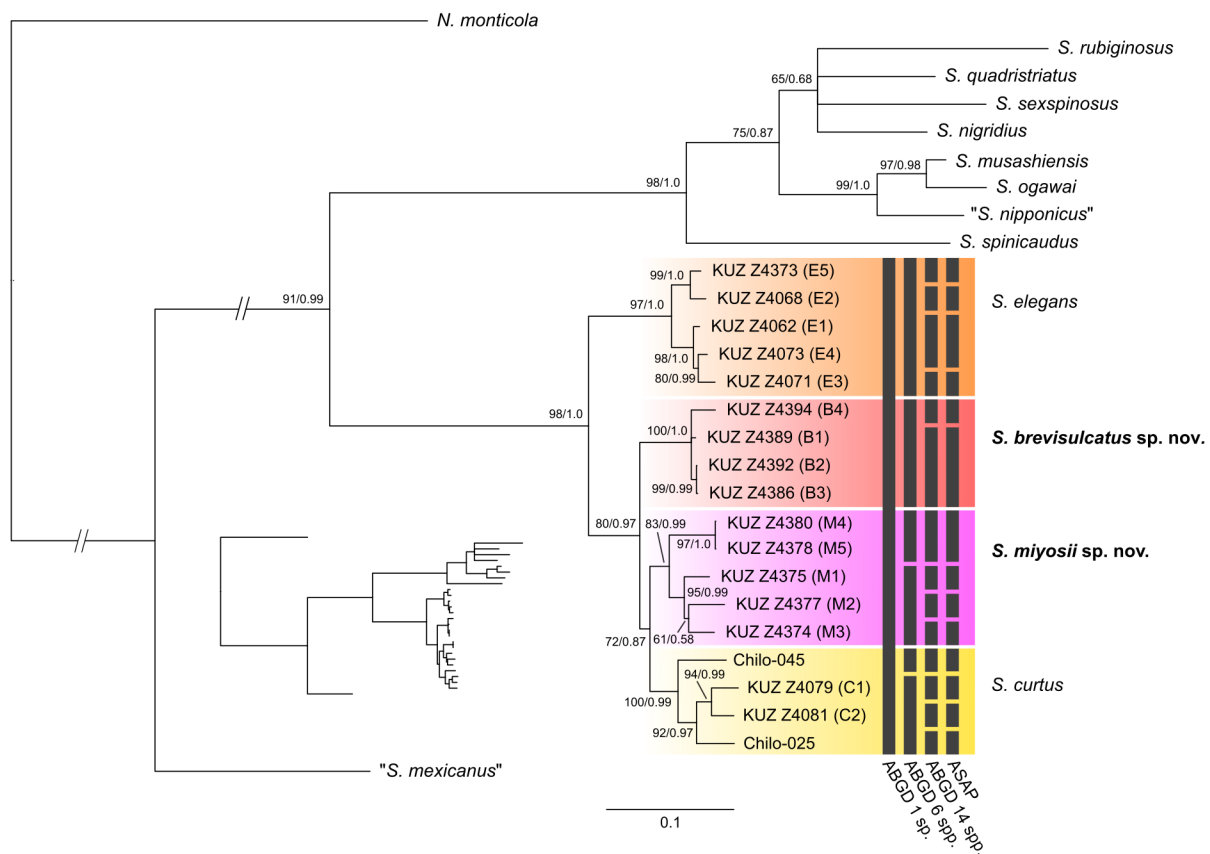


Fig. 2. Bayesian inference tree (mean $\ln L = -9352.57$) for 2008 bp-aligned positions of the ITS2, 28S and COI sequences of species of *Scolopocryptops* Newport, 1844. Inset shows real branch length. Numbers on nodes indicate ultrafast bootstrap values and Bayesian posterior probabilities. Locality numbers (E1–E5, M1–M5, B1–B4, C1 and C2) are shown in Fig. 1 and Table 1. Bars on the right show the species delimitation results of ABGD and ASAP for COI sequences.

Table 2. Uncorrected pairwise distances for 654 bp of the COI sequences of the two new species and the most closely related congeners with associated collection locality numbers (see Figs 1–2 and Table 1).

Species	Voucher	#	Number of base substitutions per site (%)																	
<i>S. elegans</i>	KUZ	Z4062	Z4062	Z4068	Z4071	Z4073	Z4373	Z4375	Z4377	Z4374	Z4380	Z4378	Z4389	Z4392	Z4386	Z4394	Z4079	Z4081	Chilo-025	
	KUZ	Z4068	5.43																	
	KUZ	Z4071	3.73	5.28																
	KUZ	Z4073	1.41	5.48	3.91															
	KUZ	Z4373	4.55	3.13	4.55	4.89														
<i>S. miyosii</i> sp. nov. (Kyushu)	KUZ	Z4375	11.29	10.81	9.70	11.45	10.42													
	KUZ	Z4377	9.94	9.97	9.35	10.19	9.43	5.88												
	KUZ	Z4374	10.36	9.58	9.26	10.60	9.34	6.11	6.61											
	KUZ	Z4380	10.22	9.63	9.32	10.80	9.56	8.27	7.68	7.69										
<i>S. miyosii</i> sp. nov. (Amami Isl.)	KUZ	Z4378	10.22	9.63	9.32	10.80	9.56	8.27	7.68	7.69	0.00									
	KUZ	Z4389	9.87	8.81	9.12	10.62	8.41	9.02	9.02	8.11	8.67	8.67								
<i>S. brevisulcatus</i> sp. nov.	KUZ	Z4392	10.95	9.84	10.16	11.59	9.44	9.92	10.02	8.51	9.21	9.21	0.96							
	KUZ	Z4386	10.99	10.02	10.18	11.63	9.45	9.93	10.03	8.50	9.21	9.21	0.98	0.16						
	KUZ	Z4394	11.25	10.55	10.73	11.42	9.08	10.98	10.73	9.97	9.86	9.86	2.80	3.32	3.39					
	KUZ	Z4079	9.83	10.45	9.20	9.86	9.12	10.49	9.55	9.94	9.05	9.05	9.79	10.32	10.34	9.69				
	KUZ	Z4081	11.99	11.21	11.06	12.05	10.52	10.17	10.00	10.55	9.66	9.66	10.88	11.59	11.79	11.07	5.93			
<i>S. curtus</i>	SYSU	Chilo-025	10.53	10.25	9.94	10.64	9.09	10.97	8.91	10.52	9.63	9.63	10.53	11.11	10.99	11.76	6.08	6.70		
	SYSU	Chilo-045	9.91	10.09	9.63	10.33	9.25	9.70	8.76	10.83	8.10	8.10	9.91	10.95	10.99	11.42	8.89	8.72	7.95	

with strong support (UFBoot = 100%, BPP = 0.99); the monophyly of *S. miyosii* was well supported only in BI analysis (UFBoot = 83%, BPP = 0.99). Within *S. miyosii*, two clades were recovered with strong support, which corresponded to the specimens from Kyushu (UFBoot = 95%, BPP = 0.99) and Amami Island (UFBoot = 97%, BPP = 1.0).

The COI pairwise distances within *S. elegans*, *S. curtus*, *S. miyosii* sp. nov., and *S. brevisulcatus* sp. nov. were 1.41–5.48%, 5.93–8.89%, 0–8.27%, and 0.16–3.39%, respectively (Table 2). Interspecific divergence ranged from 8.1% to 12.05%, with the lowest being observed between *S. miyosii* and *S. curtus* (8.1–10.97%), and the highest observed between *S. elegans* and *S. curtus* (9.09–12.05%) (Table 2).

In the ABGD analysis, *S. elegans*, *S. curtus*, *S. miyosii* sp. nov., and *S. brevisulcatus* sp. nov. were classified into a single candidate species for $P > 3.5\%$, and the presence of six and 14 species were indicated for smaller P values (Fig. 2). For $1.2\% < P < 3.5\%$, two putative species were detected within *S. curtus* specimens, each corresponding to the individuals from (Iriomote Island+northern region of Taiwan) and southern Taiwan, and *S. miyosii* was also classified into two candidate species, which corresponded to the specimens from Kyushu and Amami Island; *S. elegans* and *S. brevisulcatus* were recognized as single species. For $P < 1.1\%$, each of the *S. curtus* individuals were identified as distinct species, and *S. elegans*, *S. miyosii*, and *S. brevisulcatus* were also split into four, four, and two candidate species, respectively (Fig. 2). ASAP assigned the best score to the hypothesis of 14 species, providing the same delimitation result as in ABGD (Fig. 2).

Taxonomy

Order Scolopendromorpha Pocock, 1895
Family Scolopocryptopidae Pocock, 1896
Genus *Scolopocryptops* Newport, 1844

Scolopocryptops miyosii sp. nov.

[urn:lsid:zoobank.org:act:3BED6271-ED7E-4CAA-8F69-1DC48A68D7E1](https://zoobank.org/act:3BED6271-ED7E-4CAA-8F69-1DC48A68D7E1)

Figs 3–8

Otocryptops curtus – Miyosi 1961: 180–181; 1971: 734.

Diagnosis

Antenna with sparse minute hairs and short setae on dorsal surface of basal two or three articles, subsequent articles densely setose. Cephalic plate with short lateral marginal sulci in posterior half.

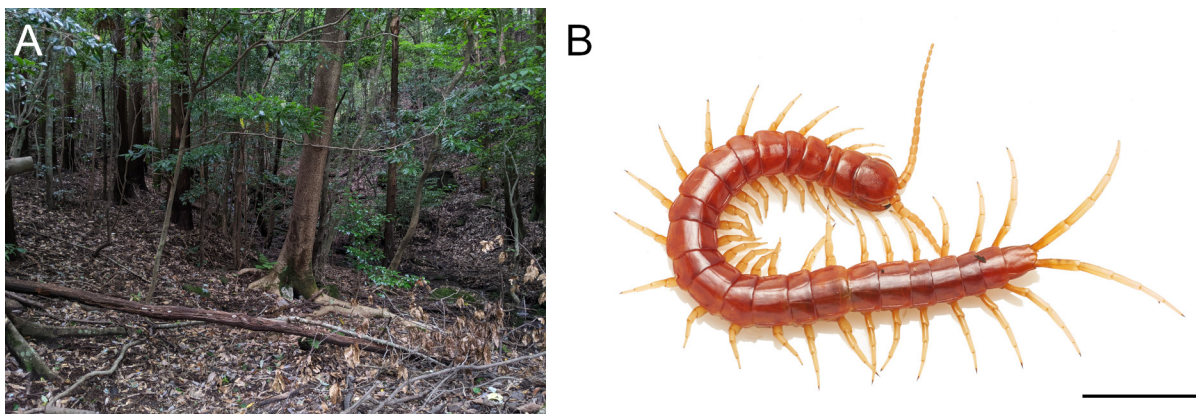


Fig. 3. *Scolopocryptops miyosii* sp. nov., paratype, ♂ (KUZ Z4376) and habitat at the type locality. **A.** Habitat (laurel tree forest) in Kagoshima, Kyushu. **B.** Live specimen, dorsal view. Scale bar = 10 mm.

Forcipular coxosternite with anterior margin weakly bilobed, bearing darkly sclerotized bands almost reaching outer part, with a pair of small teeth. Coxopleuron approx. 1.5–1.7 × as long as sternite 23; pleural dorsal margin slightly protruding from lateral margin of tergite 23, posterior and ventral margins forming approx. 70–80° angle; coxopleural process short.

Etymology

The specific name is dedicated to the late Dr Yasunori Miyosi, who first provided detailed taxonomic accounts for this new species.

We herein suggest a Japanese name for this species as ‘Miyosi-akamukade’.

Material examined

Holotype

JAPAN – **Kyushu** • ♂; Kagoshima, near Kirishima Mountains (Figs 1, 3A); 31.88765° N, 130.83962° E; 616 m alt.; 2 Aug. 2022; T. Jonishi leg.; KUZ Z4375.

Paratypes

JAPAN – **Kyushu** • 1 ♂; same locality as for holotype; 31.88796° N, 130.84037° E; 626 m alt.; 2 Aug. 2022; T. Jonishi leg.; KUZ Z4376 • 1 ♀; Kagoshima, Aira; 31.86924° N, 130.59942° E; 364 m alt.; 2 Aug. 2022; T. Jonishi leg.; KUZ Z4377.

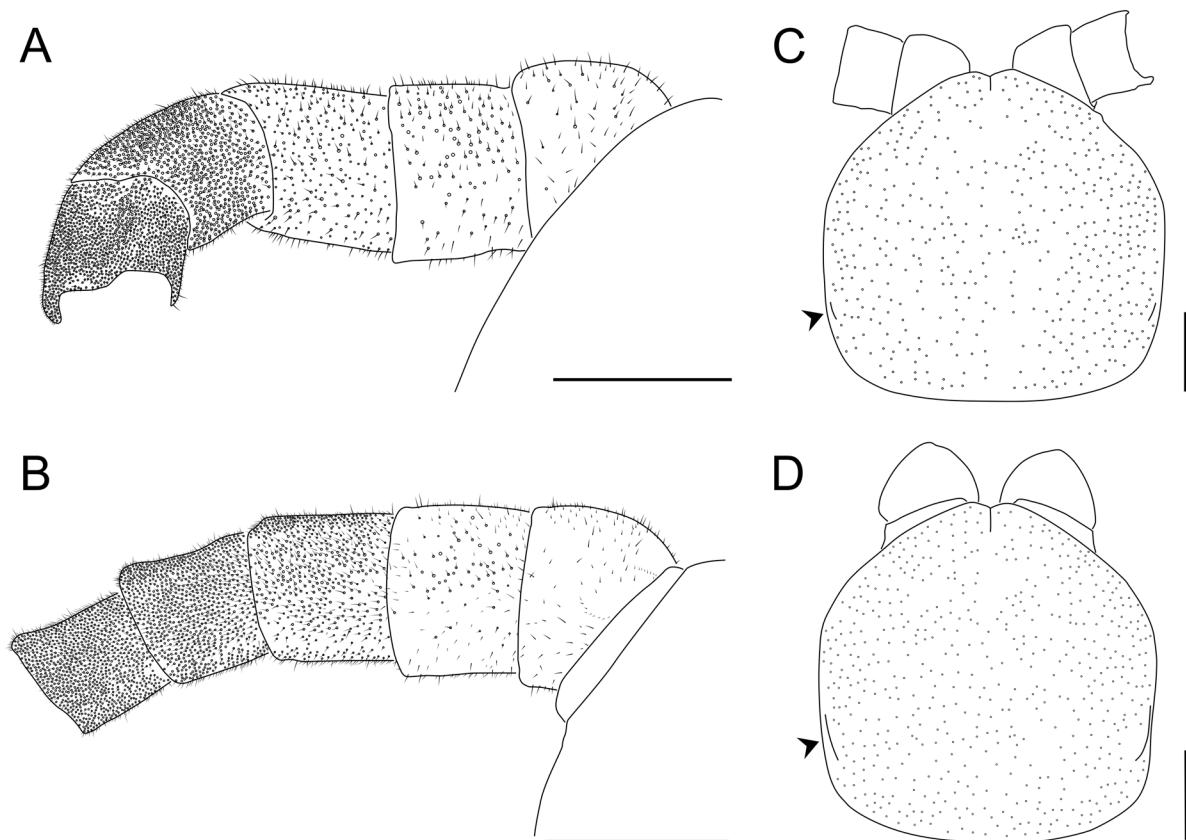


Fig. 4. *Scolopocryptops miyosii* sp. nov. **A, C.** Holotype, ♂ (KUZ Z4375). **B, D.** Paratype, ♀ (KUZ Z4377). **A–B.** Basal articles of left antenna, dorsal view. **C–D.** Cephalic plate, dorsal view; arrowheads indicate left cephalic marginal sulcus. Scale bars = 1 mm.

Additional material

JAPAN – **Kyushu** • 1 subadult; Oita, Saeki; 32.93942° N, 131.72764° E; 71 m alt.; 20 Jun. 2022; Naoto Sawada leg.; KUZ Z4374. – **Amami Island** • 1 subadult; Uken; 28.28792° N, 129.31997° E; 435 m alt.; 13 Mar. 2021; Futaro Okuyama leg.; KUZ Z4378 • 1 subadult; Uken, Mt. Yuwan-dake; 28.28962° N, 129.31441° E; 506 m alt.; 20 Jun. 2022; T. Jonishi leg.; KUZ Z4379 • 2 subadults; Yamato; 28.33112° N, 129.36187° E; 315 m alt.; 20 Jun. 2022; T. Jonishi leg.; KUZ Z4380, Z4381 • 1 ♀; same locality as for preceding; 28.33104° N, 129.36158° E; 314 m alt.; 21 Jun. 2022; T. Jonishi leg.; KUZ Z4382 • 1 subadult; same locality as for preceding; 28.33090° N, 129.36163° E; 317 m alt.; 22 Jun.

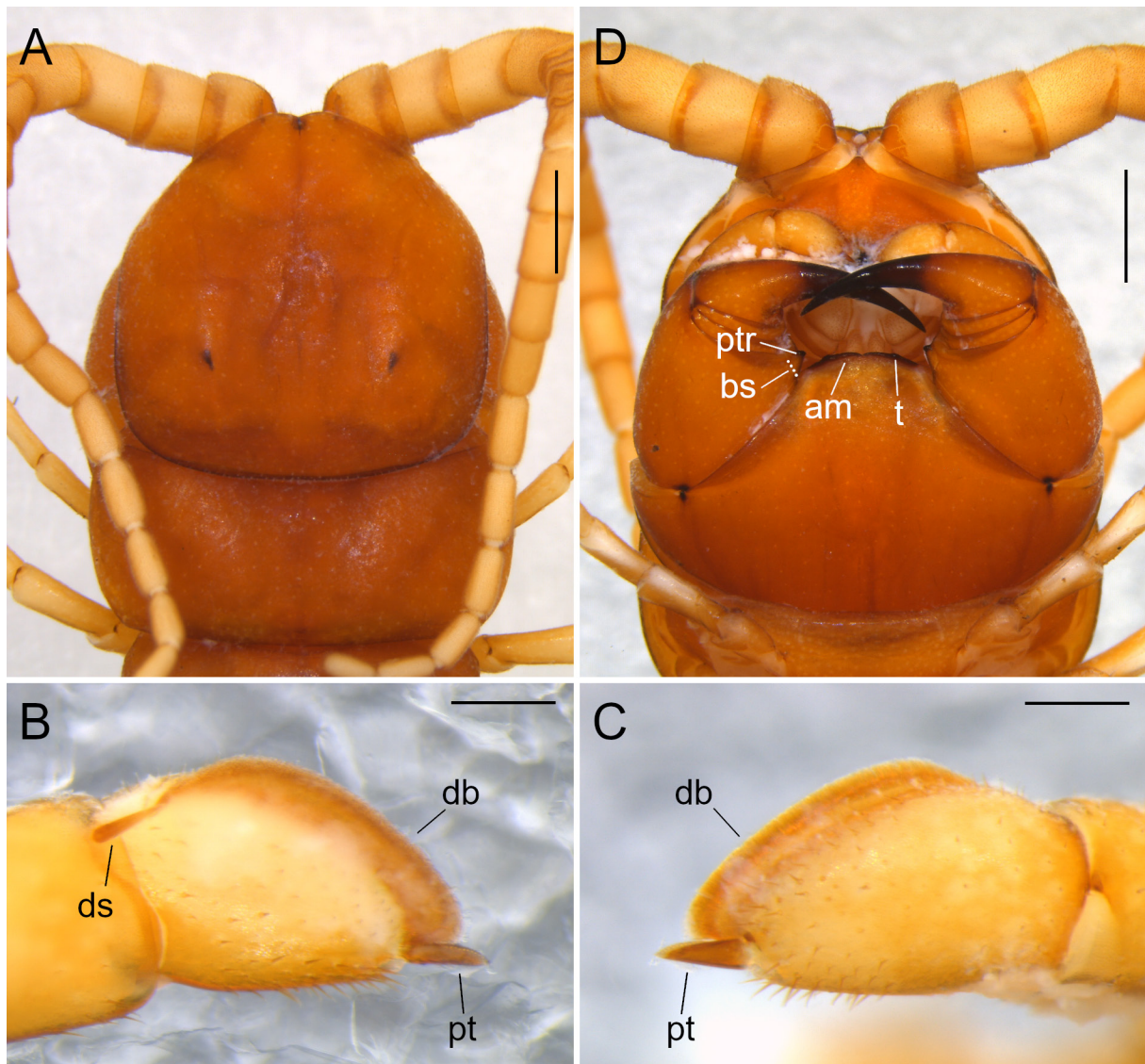


Fig. 5. *Scolopocryptops miyosii* sp. nov., holotype, ♂ (KUZ Z4375). **A.** Cephalic plate and tergite 1, dorsal view. **B.** Distal part of article 2, article 3, and pretarsus of left second maxilla, medial view. **C.** Article 3 and pretarsus of left second maxilla, lateral view. **D.** Head, ventral view. Abbreviations: am = anterior margin of forcipular coxosternite; bs = basal suture on forcipular trochanteroprefemoral process; db = dorsal brush on article 3 of second maxilla; ds = dorsal spur on article 2 of second maxilla; pt = pretarsus of second maxilla; ptr = process of forcipular trochanteroprefemur; t = tooth on anterior margin of forcipular coxosternite. Scale bars: A, D = 1 mm; B–C = 0.2 mm.

2022; T. Jonishi leg.; KUZ Z4383 • 1 ♀; same locality as for preceding; 28.33040° N, 129.36076° E; 301 m alt.; 22 Jun. 2022; T. Jonishi leg.; KUZ Z4384.

Description of holotype [variation in other specimens given in square brackets]

Body length 54.4 mm [48.0–69.1 mm in adults] in 80% ethanol, 60.3 mm [54.6–73.4 mm] before fixation. Body color brownish orange, antennae, legs, and ultimate legs yellowish (Fig. 3B).

Antennae 10.0 mm in length, approx. $0.18 \times$ [0.16–0.23 \times] as long as body, composed of 17 articles; basal 3 articles with sparse minute hairs (see Bonato *et al.* 2010) and short setae dorsally, 4th and subsequent articles densely setose [3rd article moderately setose, articles 4–17 more densely setose in KUZ Z4377 and Z4382] (Fig. 4A–B). Cephalic plate as long as wide, with sides converging anteriorly (Figs 4C–D, 5A); its surface finely punctate [minute setae on each punctum present in KUZ Z4382 and subadults]; short lateral marginal sulci present in posterior half [marginal sulci significantly longer and more apparent in KUZ Z4377] (Figs 4C–D, 5A).

Second maxillae article 2 with elongated and semi-transparent dorsal spur distally; dorsal brush without transparent margin (Fig. 5B–C); pretarsus consisting of dark brown basal and semi-transparent short apical parts (Fig. 5B–C). Forcipular coxosternite and trochanteroprefemora sparsely punctate, coxosternite without sutures (Fig. 5D); forcipular trochanteroprefemur with small and blunt black process, with apparent basal suture (Figs 5D, 6); anterior margin of coxosternite weakly convex and divided by median diastema; darkly sclerotized bands almost reaching outer part of anterior margin of coxosternite, with a pair of small but prominent teeth at middle of each side [right tooth absent in KUZ Z4377] (Figs 5D, 6).

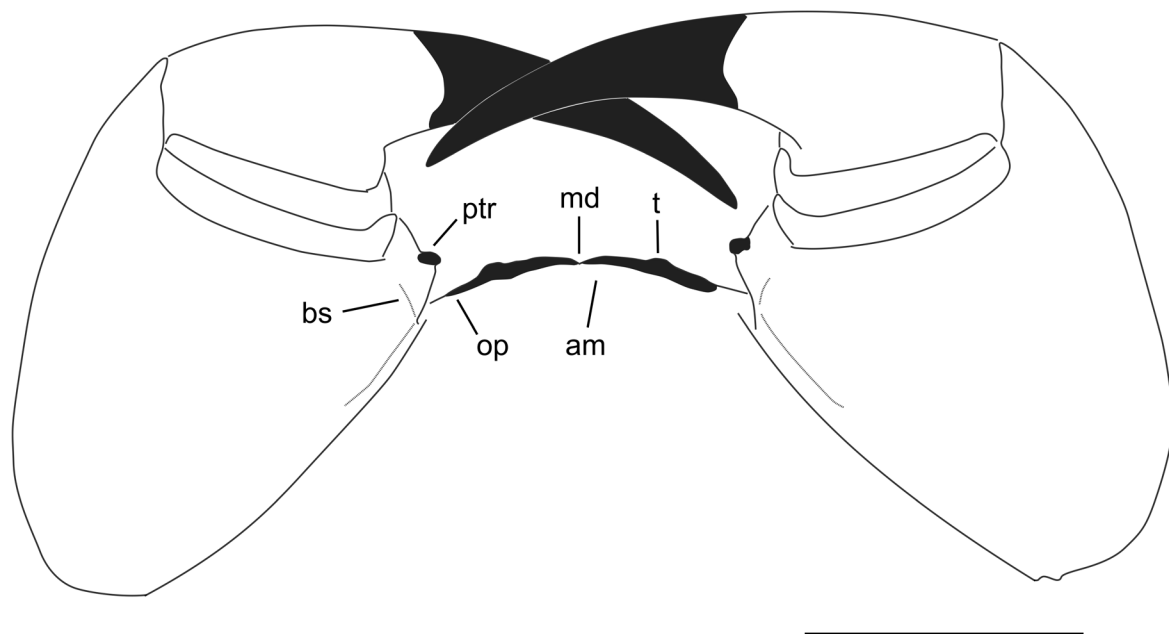


Fig. 6. *Scolopocryptops miyosii* sp. nov., holotype, ♂ (KUZ Z4375). Forcipules and coxosternite, ventral view. Abbreviations: am = anterior margin of forcipular coxosternite; bs = basal suture on forcipular trochanteroprefemoral process; md = median diastema; op = outer part of anterior margin of forcipular coxosternite; ptr = process of forcipular trochanteroprefemur; t = tooth on anterior margin of forcipular coxosternite. Scale bar = 1 mm.

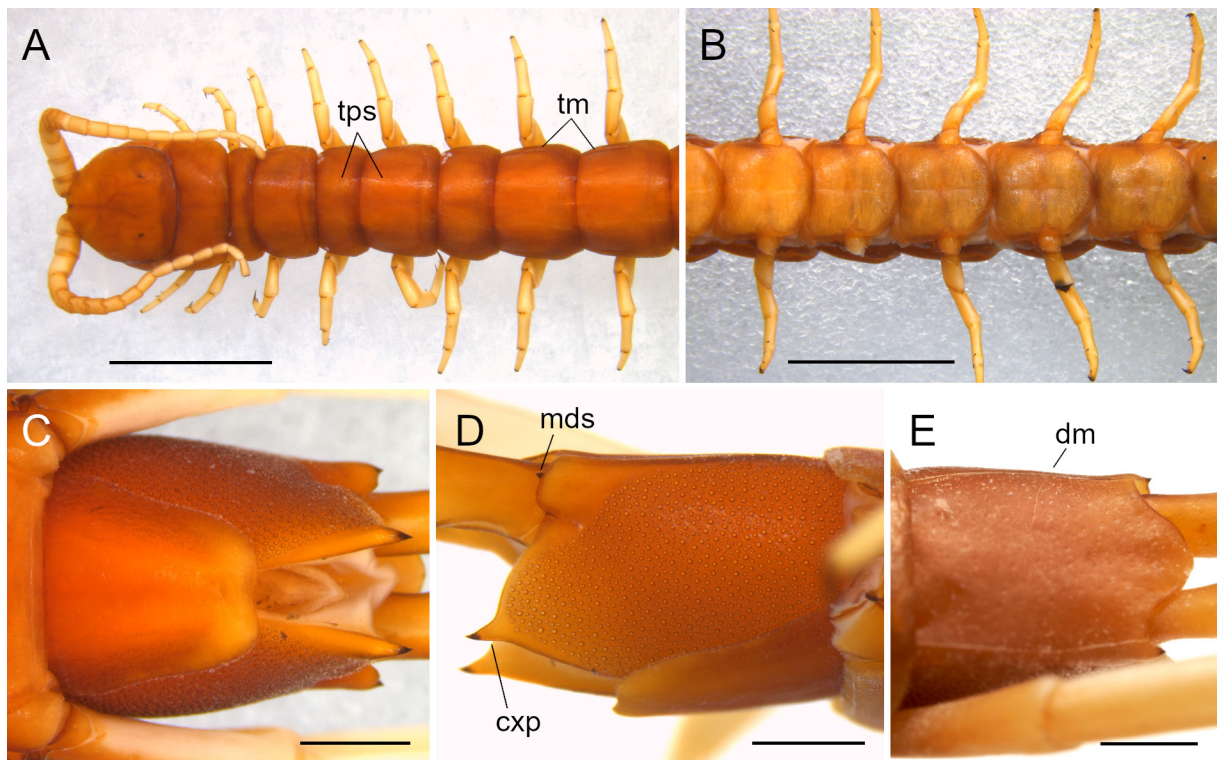


Fig. 7. *Scolopocryptops miyosii* sp. nov., holotype, ♂ (KUZ Z4375). **A.** Cephalic plate and tergites 1–8, dorsal view. **B.** Sternites 10–14, ventral view. **C.** Sternite 23, ventral view. **D.** Right coxopleuron, lateral view. **E.** Tergite 23, dorso-lateral view. Abbreviations: cxp = coxopleural process; dm = dorsal margin of ultimate pleuron; mds = minute dark spine on ultimate pleuron; tm = tergal margination; tps = tergal paramedian suture. Scale bars: A–B = 5 mm; C–E = 1 mm.

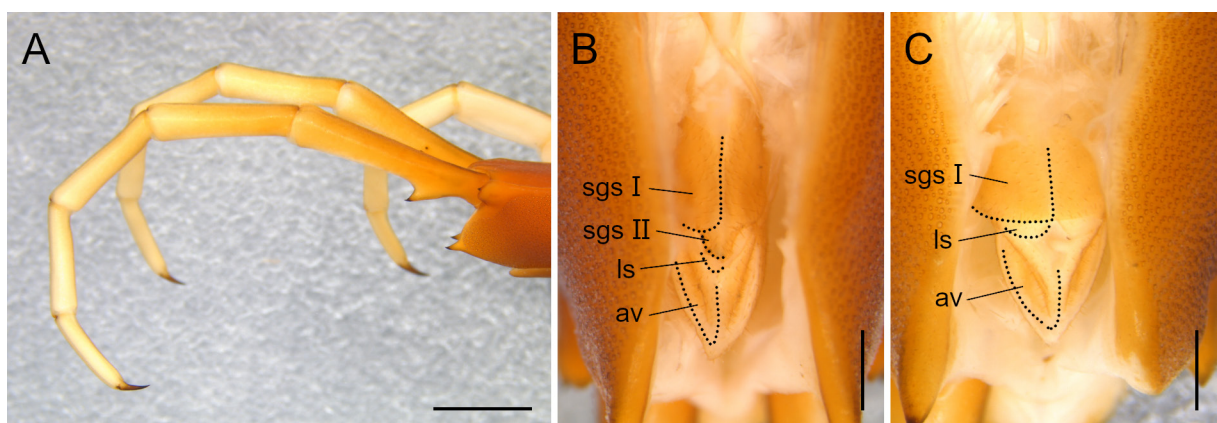


Fig. 8. *Scolopocryptops miyosii* sp. nov. **A–B.** Holotype, ♂ (KUZ Z4375). **C.** Paratype, ♀ (KUZ Z4377). **A.** Right ultimate leg, lateral view. **B.** Male genital segments, lamina subanalis, and anal valves, ventral view. **C.** Female genital segment, lamina subanalis, and anal valves, ventral view. Abbreviations: av = anal valve; ls = lamina subanalis; sgs I = sternite of genital segment 1; sgs II = sternite of genital segment 2. Scale bars: A = 2 mm; B–C = 0.5 mm.

Tergites finely punctate; tergite 1 with anterior transverse suture, anterior margin covered by cephalic plate (Figs 5A, 7A). Paramedian sutures present on tergites 2–22 (Fig. 7A); lateral marginations complete on tergites 6–21 (Fig. 7A).

Sternites lacking paramedian sutures, finely punctate (Fig. 7B); sternites 3–20 with shallow longitudinal sulcus and slight median depression (Fig. 7B), both shallower and unapparent on anterior sternites. Sides of sternite 23 converging posteriorly, its posterior margin slightly concave (Fig. 7C).

Spiracles ovoid, present on leg-bearing segments 3, 5, 8, 10, 12, 14, 16, 18, 20, and 22.

Legs lacking setae; tarsi of legs 1–21 undivided; legs 1–19 [1–20 in KUZ Z4376] with lateral and ventral tibial spurs and tarsal spur, legs 20 and 21, respectively, with tibial spur and tarsal spur [leg 21 without tibial spur in KUZ Z4382]; leg 22 without spurs. All legs with two accessory spines.

Coxopleuron approx. $1.7 \times [1.5–1.7 \times]$ as long as sternite 23 (Fig. 7D). Dorsal margin of ultimate pleuron slightly protruding from lateral side of tergite 23 (Fig. 7D–E), posterior margin with minute dark spine (Fig. 7D). Posterior and ventral margins of coxopleuron converging posteriorly, forming approx. $80^\circ [70–80]$ angle (Fig. 7D); coxopleural process short, tip of process pointed, slightly directed dorsally (Fig. 7D). Surface of coxopleuron without setae, covered with various sized coxal pores; coxopleural process and dorso-posterior area of coxopleuron poreless (Fig. 7D).

Ultimate leg 14.1 mm [13.9–17.3 mm] in length, $0.26 \times [0.24–0.3 \times]$ as long as body; all articles lacking setae (Fig. 8A); prefemur with two conical and pointed spinose processes, ventral process large, dorso-medial one minute; pretarsus with two short accessory spines.

Genital segments occupying approx. $\frac{1}{2}$ length of sternite 23. Sternite of genital segment 1 with sparse minute setae; posterior margin weakly convex (Fig. 8B). Sternite of genital segment 2 well developed, covered with sparse minute setae; posterior part of genital segment 2 overlapped by lamina subanalis, penis not visible in ventral view (Fig. 8B); lamina subanalis situated between genital segment 2 and anal valves (Fig. 8B) [in female paratype KUZ Z4377, genital segment 1 as described for holotype, genital segment 2 absent; lamina subanalis situated between genital segment 1 and anal valves] (Fig. 8C).

Remarks

This species has previously been identified as *S. curtus* (Miyosi 1961, 1971; Ogawa 1961), but *S. miyosii* sp. nov. can be distinguished by the following characters: the presence of short sulci along the lateral margin of the cephalic plate (Fig. 4C–D) (vs sulci absent in *S. curtus*), the convex anterior margin of the forcipular coxosternite with teeth (Figs 5D, 6) (vs anterior margin virtually straight with teeth almost reduced, forming antero-lateral corner of sclerotized bands; also see Remarks for *S. brevisulcatus* sp. nov. below), and the dorsal margin of the ultimate pleuron protruding from the lateral side of tergite 23 (Fig. 7E) (vs dorsal margin flattened) (see Table 3).

Distribution

Known from Kyushu, and Amami Island in the Ryukyu Islands.

Scolopocryptops brevisulcatus sp. nov.

[urn:lsid:zoobank.org:act:3C9DB52B-2691-4980-B339-1B31E177F10C](https://zoobank.org/act:3C9DB52B-2691-4980-B339-1B31E177F10C)

Figs 9–14

Diagnosis

Antenna with sparse minute hairs and short setae on dorsal surface of basal four articles, subsequent articles densely setose. Cephalic plate with short and shallow lateral marginal sulci in posterior half.

Forcipular coxosternite with anterior margin slightly bilobed but median diastema almost lacking, darkly sclerotized bands not reaching outer part of anterior margin, with a pair of almost-reduced teeth. Coxopleuron approx. 1.6–1.7 × as long as sternite 23; pleural dorsal margin slightly protruding from lateral margin of tergite 23, posterior and ventral margins forming approx. 70–80° angle; coxopleural process short.

Etymology

The specific name is derived from the Latin words ‘*brevis*’ (‘short, shallow’) and ‘*sulcus*’ (‘groove’), referring to the unapparent cephalic marginal sulcus of this new species.

We herein suggest a Japanese name for this species as ‘Kirekomi-akamukade’.

Material examined

Holotype

JAPAN – **Okinawa Island** • ♂; Motobu, near Mt. Katsuu-dake (Figs 1, 9A); 26.63157° N, 127.93771° E; 311 m alt.; 14 Jun. 2022; T. Jonishi leg.; KUZ Z4390.

Paratypes

JAPAN – **Okinawa Island** • 1 subadult; Kunigami, near Mt. Nishime-dake; 26.80745° N, 128.26618° E; 298 m alt.; 4 May 2021; F. Okuyama leg.; KUZ Z4386 • 1 adult, sex undetermined; same locality as for preceding; 26.81195° N, 128.28415° E; 107 m alt.; 8 Apr. 2022; F. Okuyama leg.; KUZ Z4387 • 1 ♀; same collection data as for holotype; KUZ Z4389 • 1 ♂; Kunigami, near Mt. Nishime-dake; 26.80080° N, 128.27728° E; 355 m alt.; 15 Jun. 2022; T. Jonishi leg.; KUZ Z4391 • 1 subadult; Kunigami, Mt. Fuenchiji; 26.75251° N, 128.24303° E, 384 m alt.; 16 Jun. 2022; T. Jonishi leg.; KUZ Z4392.

Additional material

JAPAN – **Okinawa Island** • 1 adult, sex undetermined; same locality as for holotype; 26.63145° N, 127.93812° E; 291 m alt.; 20 Sep. 2019; T. Jonishi leg.; KUZ Z4385 • 1 subadult; same locality as for holotype; 26.63139° N, 127.93792° E; 307 m alt.; 14 Jun. 2022; T. Jonishi leg.; KUZ Z4388 • 1 juv.; Ogimi, near Mt. Nekumachiji; 26.68491° N, 128.13430° E; 244 m alt.; 16 Jun. 2022; T. Jonishi leg.; KUZ Z4393. – **Izena Island** • 1 ♀; Mt. Ufu-yama; 26.94288° N, 127.92713° E; 48 m alt.; 8 Nov. 2022; Ryobu Fukuyama leg.; KUZ Z4394.

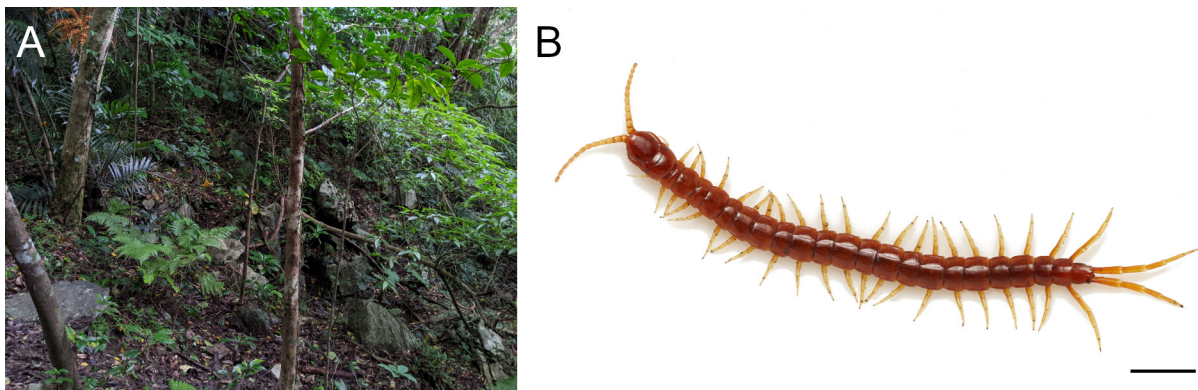


Fig. 9. *Scolopocryptops brevisulcatus* sp. nov., holotype, ♂ (KUZ Z4390) and habitat at the type locality. **A.** Habitat (laurel tree forest) on Okinawa Island. **B.** Live specimen, dorsal view. Scale bar = 10 mm.

Description of holotype [variation in other specimens given in square brackets]

Body length 58.0 mm [43.6–59.1 mm in adults] in 80% ethanol, 64.0 mm before fixation. Body color brownish red [brownish orange]; antennae, legs, and ultimate legs yellowish (Fig. 9B).

Antennae damaged, 13th and subsequent articles lost [9.9 mm in length, approx. 0.2 × as long as body, composed of 17 articles in paratype KUZ Z4391]; density of setae increasing toward distal articles; basal 4 articles with sparse minute hairs (see Bonato *et al.* 2010) and short setae dorsally, 5th and subsequent articles setose, 6th–17th articles more densely covered with setae [basal 2 articles sparsely setose, 3rd and subsequent articles densely covered with setae in juvenile KUZ Z4393; 4th article moderately setose, 5th–17th articles more densely covered with setae in subadults] (Fig. 10A). Cephalic plate as long as wide, sides converging anteriorly (Figs 10B, 11A); its surface finely punctate [minute setae on each punctum present in juvenile and subadults]; short and shallow lateral marginal sulci present in posterior half [marginal sulci absent in juvenile and subadults] (Figs 10B, 11A).

Second maxillae article 2 with elongated and semi-transparent dorsal spur distally; dorsal brush without transparent margin (Fig. 11B–C); pretarsus consisting of dark brown basal and semi-transparent short apical parts (Fig. 11B–C). Forcipular coxosternite and trochanteroprefemora sparsely punctate, coxosternite without sutures (Fig. 11D); forcipular trochanteroprefemur with small and blunt black process, with apparent basal suture (Figs 11D, 12); anterior margin of coxosternite almost straight and slightly bilobed but median diastema almost lacking; darkly sclerotized bands not reaching outer part of anterior margin of coxosternite; a pair of teeth almost reduced, forming antero-lateral corner of sclerotized bands [teeth on anterior margin prominent in juvenile and subadults] (Figs 11D–E, 12).

Tergites finely punctate; tergite 1 with anterior transverse suture, anterior margin covered by cephalic plate (Figs 11A, 13A). Paramedian sutures present on tergites 2–22, lateral marginations complete on tergites 6–21 (Fig. 13A).

Sternites lacking paramedian sutures, finely punctate (Fig. 13B); sternites 2–20 with shallow longitudinal sulcus and slight median depression (Fig. 13B), both shallower and unapparent on anterior sternites. Sternite 23 damaged, right posterior margin lost [sides of sternite 23 converging posteriorly, posterior margin slightly concave in paratype KUZ Z4387 and other specimens] (Fig. 13C).

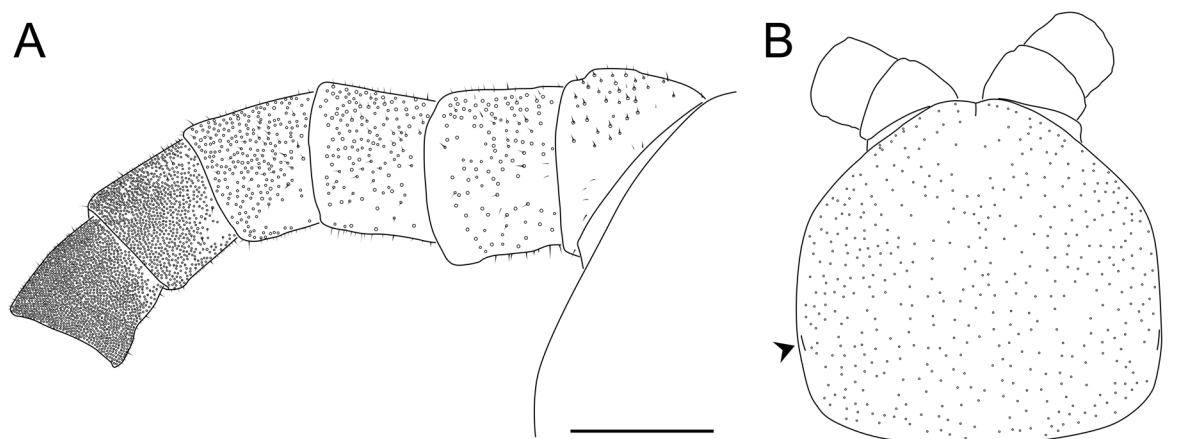


Fig. 10. *Scolopocryptops brevisulcatus* sp. nov., holotype, ♂ (KUZ Z4390). **A.** Basal articles of left antenna, dorsal view. **B.** Cephalic plate, dorsal view; arrowhead indicates left cephalic marginal sulcus. Scale bars = 1 mm.

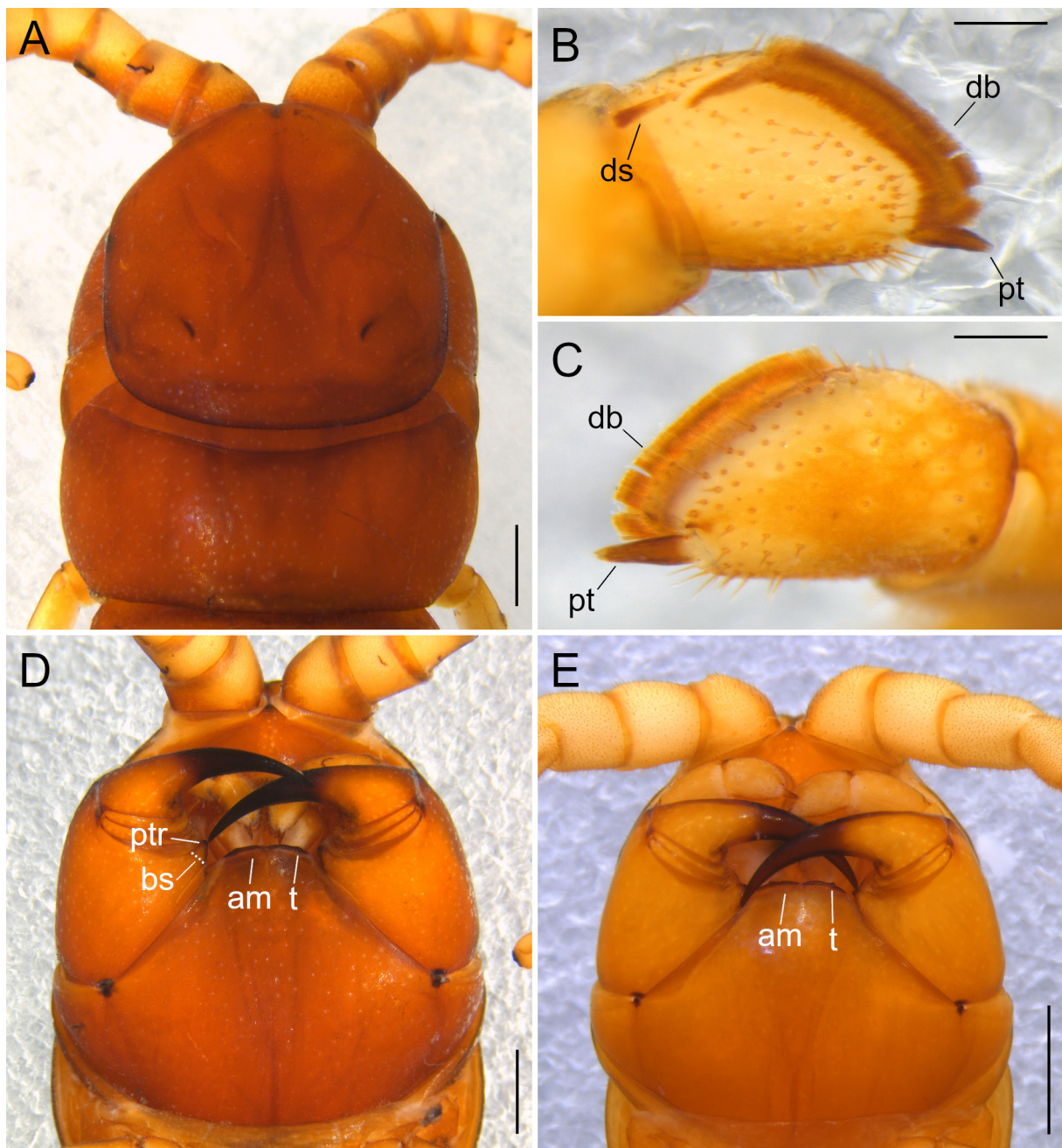


Fig. 11. *Scolopocryptops brevisulcatus* sp. nov. **A–D.** Holotype, ♂ (KUZ Z4390). **E.** Paratype, subadult, sex undetermined (KUZ Z4386). **A.** Cephalic plate and tergite 1, dorsal view. **B.** Distal part of article 2, article 3, and pretarsus of left second maxilla, medial view. **C.** Article 3 and pretarsus of left second maxilla, lateral view. **D–E.** Head, ventral view. Abbreviations: am = anterior margin of forcipular coxosternite; bs = basal suture on forcipular trochanteroprefemoral process; db = dorsal brush on article 3 of second maxilla; ds = dorsal spur on article 2 of second maxilla; pt = pretarsus of second maxilla; ptr = process of forcipular trochanteroprefemur; t = tooth on anterior margin of forcipular coxosternite. Scale bars: A, D–E = 1 mm; B–C = 0.2 mm.

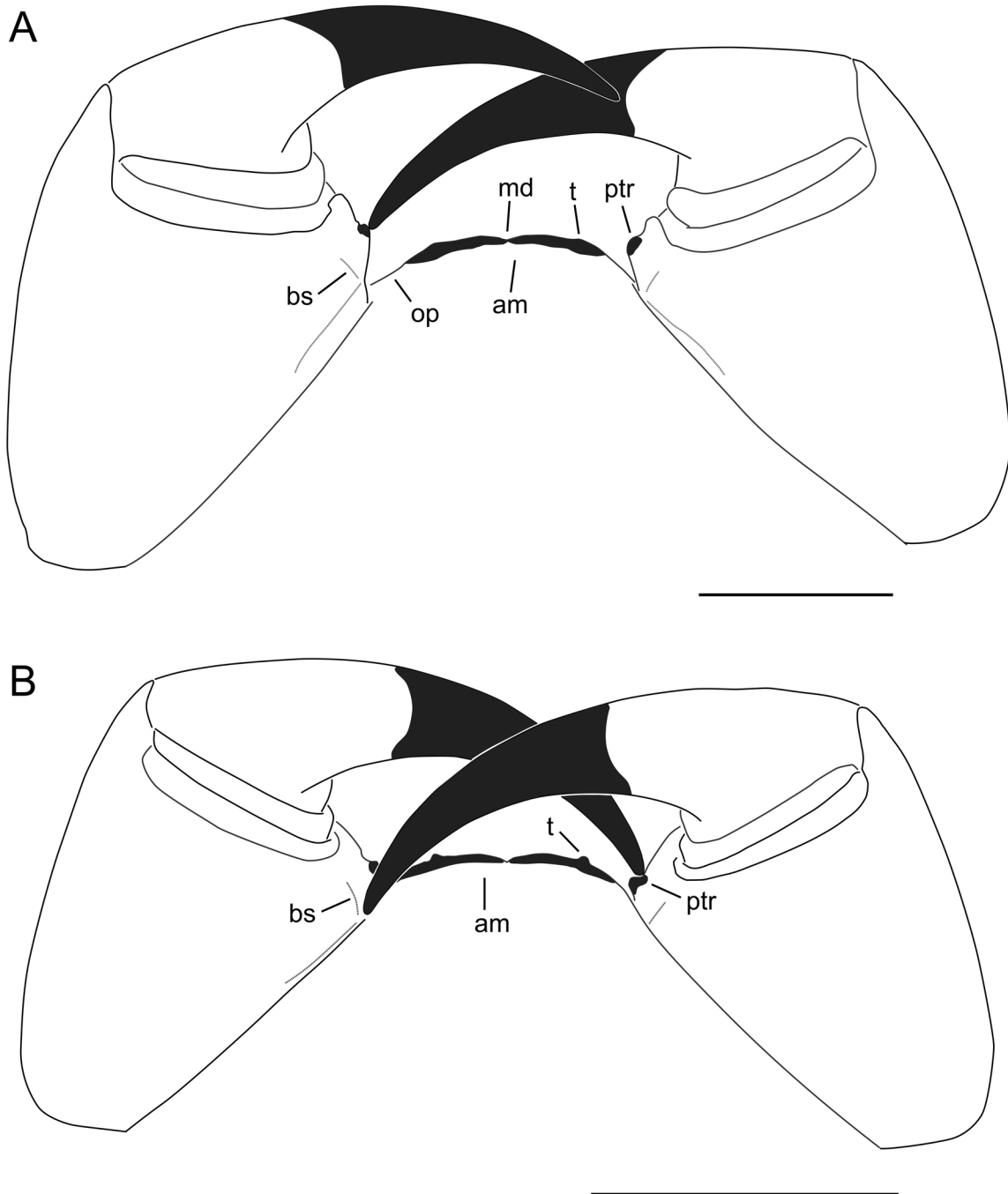


Fig. 12. *Scolopocryptops brevisulcatus* sp. nov. **A.** Holotype, ♂ (KUZ Z4390). **B.** Paratype, subadult, sex undetermined (KUZ Z4386). Forcipules and forcipular coxosternite, ventral view. Abbreviations: am = anterior margin of forcipular coxosternite; bs = basal suture on forcipular trochanteroprefemoral process; md = median diastema; op = outer part of anterior margin of forcipular coxosternite; ptr = process of forcipular trochanteroprefemur; t = tooth on anterior margin of forcipular coxosternite. Scale bars: A = 1 mm; B = 0.2 mm.

Spiracles ovoid, present on leg-bearing segments 3, 5, 8, 10, 12, 14, 16, 18, 20, and 22.

Legs lacking setae; tarsi of legs 1–21 undivided; legs 1–19 with lateral and ventral tibial spurs and tarsal spur, legs 20 and 21, respectively, with tibial spur and tarsal spur; leg 22 without spurs. All legs with two accessory spines.

Coxopleuron approx. $1.7 \times [1.6\text{--}1.7 \times]$ as long as sternite 23 (Fig. 13D). Dorsal margin of ultimate pleuron slightly protruding from lateral side of tergite 23 (Fig. 13D–E), posterior margin with minute dark spine (Fig. 13D). Posterior and ventral margins of coxopleuron converging posteriorly, forming approx. $70^\circ [70\text{--}80^\circ]$ angle (Fig. 13D); coxopleural process short, tip of process broken [tip of process pointed, slightly directed dorsally in KUZ Z4387] (Fig. 13D). Surface of coxopleuron without setae, covered with coxal pores of various size; coxopleural process and dorso-posterior area of coxopleuron poreless (Fig. 13D).

Ultimate leg 15.3 mm in length, $0.26 \times$ as long as body; all articles lacking setae (Fig. 14A); prefemur with two conical and pointed spinose processes, ventral process large, dorso-medial one minute; pretarsus with two accessory spines.

Genital segments occupying approx. $\frac{1}{2}$ length of sternite 23. Sternite of genital segment 1 with sparse minute setae; posterior margin weakly convex (Fig. 14B). Sternite of genital segment 2 well developed,

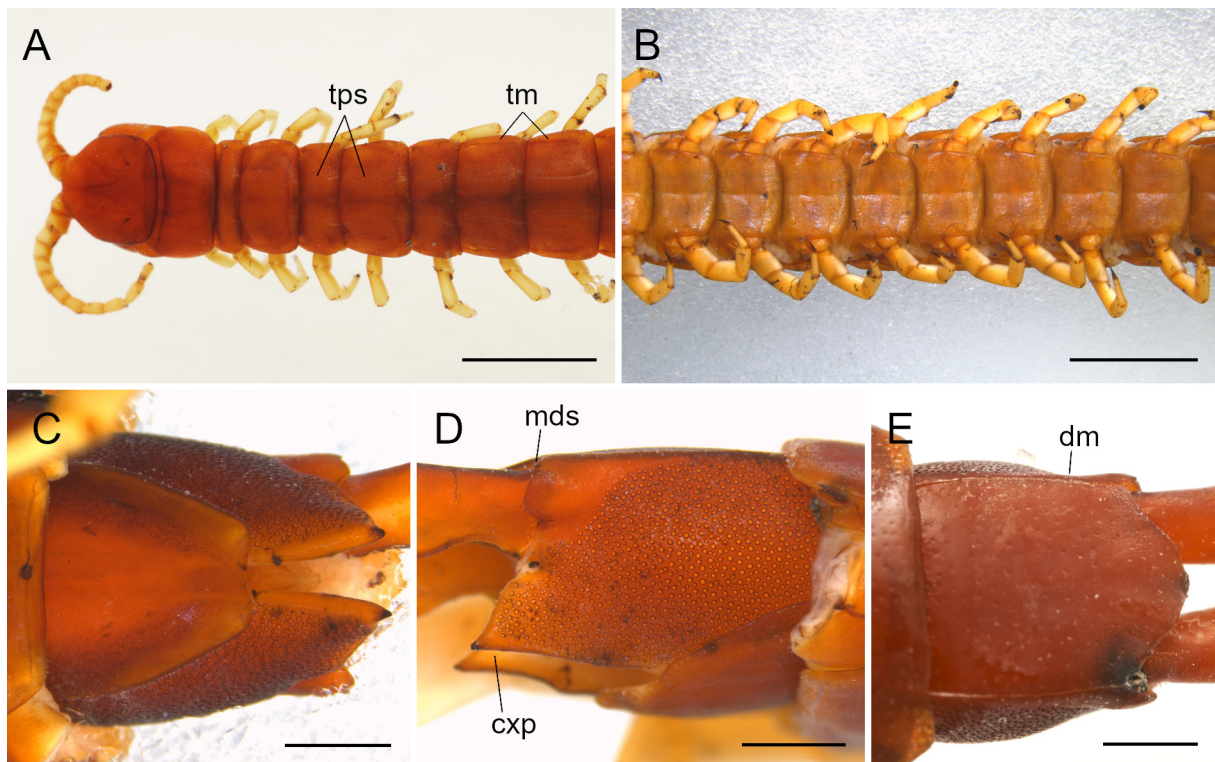


Fig. 13. *Scolopocryptops brevisulcatus* sp. nov. **A–B, D–E.** Holotype, ♂ (KUZ Z4390). **C.** Paratype, sex undetermined (KUZ Z4387). **A.** Cephalic plate and tergites 1–8, dorsal view. **B.** Sternites 10–17, ventral view. **C.** Sternite 23, ventral view. **D.** Right coxopleuron, lateral view. **E.** Tergite 23, dorsal view. Abbreviations: cxp = coxopleural process; dm = dorsal margin of ultimate pleuron; mds = minute dark spine on ultimate pleuron; tm = tergal margination; tps = tergal paramedian suture. Scale bars: A–B = 5 mm; C–E = 1 mm.

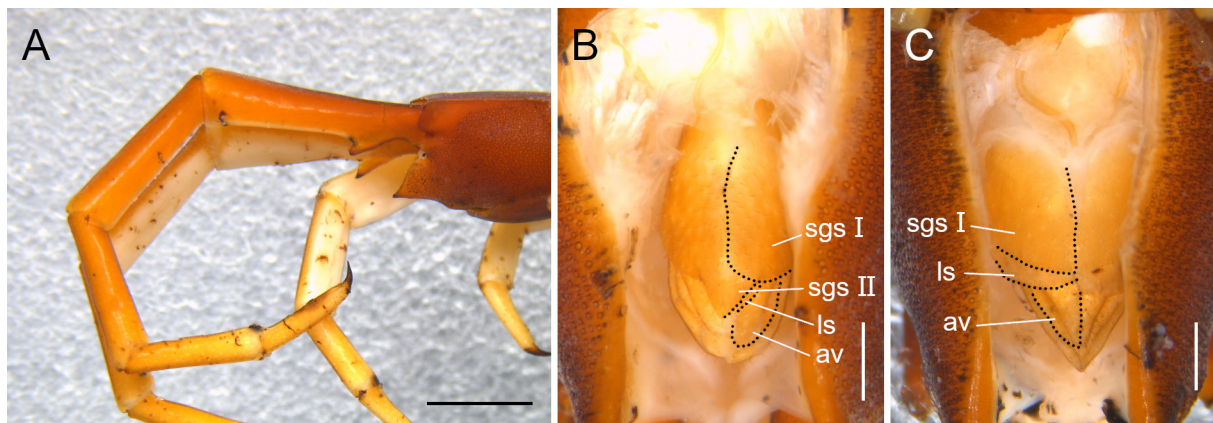


Fig. 14. *Scolopocryptops brevisulcatus* sp. nov. **A–B.** Holotype, ♂ (KUZ Z4390). **C.** Paratype, ♀ (KUZ Z4389). **A.** Right ultimate leg, lateral view. **B.** Male genital segments, lamina subanalis, and anal valves, ventral view. **C.** Female genital segment, lamina subanalis, and anal valves, ventral view. Abbreviations: av = anal valve; ls = lamina subanalis; sgs I = sternite of genital segment 1; sgs II = sternite of genital segment 2. Scale bars: A = 2 mm; B–C = 0.5 mm.

covered with sparse minute setae; posterior part of genital segment 2 overlapped by anal valves, penis not visible in ventral view (Fig. 14B); lamina subanalis situated between genital segment 2 and anal valves (Fig. 14B) [in female paratype KUZ Z4389, genital segment 1 as described for holotype, genital segment 2 absent; lamina subanalis situated between genital segment 1 and anal valves] (Fig. 14C).

Remarks

This species has previously been identified as *S. elegans* (e.g., Ômine 1987, 2002) and *S. curtus* (Ômine & Ito 1998) and is quite similar to *S. miyosii* sp. nov. (see above). However, *S. brevisulcatus* sp. nov. can be distinguished by the combination of the following features: basal 4 antennal articles of adults with sparse setae (Fig. 10A) (vs only basalmost article sparsely setose or all articles densely setose in *S. elegans*, and basal 2 or 3 articles with sparse setae in *S. miyosii*), the presence of short sulci along the lateral margin of the cephalic plate in adults (Fig. 10B) (vs sulci absent in *S. curtus*), the anterior margin of coxosternite almost lacking median diastema (Figs 11D, 12A) (vs median diastema apparent in *S. elegans*, *S. miyosii*, and *S. curtus*), the sclerotized bands of coxosternite not reaching outer part of anterior margin (Figs 11D, 12A) (vs sclerotized bands almost reaching outer part in *S. elegans* and *S. miyosii*), the almost-reduced teeth on coxosternite (Figs 11D, 12A) (vs teeth prominent in *S. miyosii*), the dorsal margin of the ultimate pleuron protruding from the lateral margin of tergite 23 (Fig. 13E) (vs dorsal margin flattened in *S. curtus*) and the short coxopleural process (Fig. 13D) (vs the process moderately long in *S. elegans*) (see Table 3).

Distribution

Known from Okinawa Island and its adjacent islet (Izena Island), Ryukyu Islands.

Discussion

The phylogenetic analyses indicated that *S. elegans*, *S. miyosii* sp. nov., *S. brevisulcatus* sp. nov., and *S. curtus* are closely related and form a clade sister to the rest of the “Asian/North American” group; the results support the recovery of *S. elegans*, *S. curtus*, and *S. brevisulcatus*, while the monophyly of *S. miyosii* was supported only in BI analysis.

Table 3. Morphological comparison of the four closely related species of *Scolopocryptops* Newport, 1844 [variations are indicated in brackets]. Diagnostic characters of *S. elegans* (Takakuwa, 1937) and *S. curtus* (Takakuwa, 1939) mainly follow Jonishi & Nakano (2022).

	<i>S. elegans</i>	<i>S. miyosii</i> sp. nov.	<i>S. brevisulcatus</i> sp. nov.	<i>S. curtus</i>
number of antennal articles with sparse setae on dorsal surface	1 [0] *	3 [2]	4 [2 or 3 in juveniles and subadults]	3 [article 4 moderately setose]**
cephalic marginal sulci	present	present	present [absent in juvenile and subadults]	absent
anterior margin of forcipular coxosternite	weakly convex and bilobed	weakly convex and bilobed	almost straight and slightly bilobed but median diastema almost lacking	virtually straight, and bilobed
sclerotized bands on anterior margin of coxosternite	almost reaching outer part of anterior margin **	almost reaching outer part of anterior margin	not reaching outer part of anterior margin	not reaching [reaching] outer part of anterior margin **
teeth on anterior margin of coxosternite	absent	present	almost reduced, forming antero-lateral corner of sclerotized bands [prominent in juvenile and subadults]	almost reduced, forming antero-lateral corner of sclerotized bands [prominent in juvenile and subadult]**
dorsal margin of ultimate pleuron	protruding from tergite 23	slightly protruding from tergite 23	slightly protruding from tergite 23	not protruding from tergite 23
angle of posterior and ventral margins of coxopleuron	approx. 60–65°	approx. 70–80°	approx. 70–80°	approx. 70–80°
coxopleural process	moderately long	short	short	short

* based on a newly collected specimen (KUZ Z4373 from Tokyo, Eastern Honshu)

** updated from Jonishi & Nakano (2022) after comparison with *S. miyosii* sp. nov. and *S. brevisulcatus* sp. nov.

The COI genetic divergence between the two lineages within *S. miyosii* sp. nov. obtained from Kyushu and Amami Island is noteworthy. The distance between these two lineages is relatively large (7.68–8.27%) compared with levels of intraspecific divergence in *S. elegans* (1.41–5.48%) and *S. brevisulcatus* sp. nov. (0.16–3.39%) but is smaller than the maximum divergence within *S. curtus* (8.89%). Based on the COI genetic distances, ABGD provided three delimitation hypotheses. The threshold values used to separate intraspecific and interspecific distances were 9.1% in the one-species hypothesis, 7.3% in the six-species hypothesis, and 2.3% in the 14-species hypothesis, which was also supported by ASAP. The 2.3% genetic distance in the 14-species hypothesis is much lower than the barcoding gap of species of *Scolopocryptops* summarized by Garrick *et al.* (2018) (around 10%), and the one-species hypothesis is discordant with the morphological differences among the specimens. The six-species hypothesis is concordant with the previously observed barcoding gap.

In this scheme, the examined specimens are classified as follows: 1) *S. elegans*, 2) the individuals from Okinawa and Iznena islands (= *S. brevisulcatus* sp. nov.), 3) the specimens from Kyushu (= *S. miyosii* sp. nov.), 4) the specimens from Amami Island (= *S. miyosii*), 5) *S. curtus* from Iriomote Island and the northern region of Taiwan, and 6) *S. curtus* sequenced from southern Taiwan. However, since no morphological differences were found among the specimens from Kyushu and Amami Island, it seems that this result over-splits geographically distant populations within a species. Although morphological features of the specimen of *S. curtus* from southern Taiwan (SYSU Chilo-045) have not been investigated in this study, the collecting locality of this specimen, Yanping in Taitung County, is close to the type locality of this species (Hengchun, southernmost Taiwan) (Fig. 1). Given that the morphological features of the specimens from Iriomote Island and northern Taiwan are consistent with those of the original description of Takakuwa (1939) (Chao & Chang 2008; Jonishi & Nakano 2022) and the monophyly of these specimens is strongly supported, it would be reasonable to treat all four specimens of “*S. curtus*” as a single species. Also considering that the distinctness of *S. elegans* and *S. brevisulcatus* is supported by both morphological and molecular data, the examined specimens are classified into four species: *S. elegans*, *S. miyosii*, *S. brevisulcatus*, and *S. curtus*.

Scolopocryptops miyosii sp. nov. and *S. brevisulcatus* sp. nov. have external features similar to those of *S. elegans* and *S. curtus*, viz., large body size, reddish body color, the absence of complete cephalic marginal sulci, the lack of a transparent margin on the dorsal brush of article 3 of the second maxilla, and the presence of sternal longitudinal sulci. The absence of complete cephalic marginal sulci and the presence of sternal sulci distinguish them from most other “Asian/North American” *Scolopocryptops*. The four species can be distinguished from each other by the combination of the following characters: number of basal antennal articles with sparse setae, presence/absence of lateral short sulci on the cephalic plate, shape of the anterior margin of the forcipular coxosternite, position of the dorsal margin of the ultimate pleuron with respect to tergite 23, angle of the posterior and ventral margins of the coxopleuron, and length of the coxopleural process (Table 3).

Scolopocryptops miyosii sp. nov., *S. brevisulcatus* sp. nov., and *S. curtus* are highly similar. Two of their diagnostic characters, the density of setae on basal antennal articles and the presence/absence of teeth on the anterior margin of the coxosternite, are variable within each species, and the presence/absence of short cephalic marginal sulci also varies within *S. brevisulcatus*. However, *S. curtus* is distinct from the two new species in that the dorsal margin of the ultimate pleuron does not protrude from tergite 23 (vs dorsal margin slightly protruding from tergite 23, Figs 7E, 13E). *Scolopocryptops miyosii* and *S. brevisulcatus* can also be distinguished from each other by the density of the antennal setae (Figs 4A–B, 10A) and the shape of the anterior margin of the coxosternite in adults (see Remarks for *S. brevisulcatus*) (Figs 5D, 6, 11D, 12A).

Previous records suggest that the ranges of *S. elegans* and *S. curtus* overlap from southern Kyushu to the southern Ryukyu Islands; however, the present results show that specimens from Kyushu and Amami Island and individuals from Izena and Okinawa islands belong to distinct species. The results indicate the allopatric distribution of the four closely related taxa: *S. elegans* ranges from Honshu to Shikoku, *S. miyosii* sp. nov. ranges from Kyushu to Amami Island, *S. brevisulcatus* sp. nov. occurs on Izena Island and Okinawa Island, and *S. curtus* ranges from the southern Ryukyus to Taiwan. By contrast, these species are often found sympatrically with other members of the Asian/North American group, e.g., *S. elegans* with *S. rubiginosus* (L. Koch, 1878) and *S. quadristriatus* (Verhoeff, 1934) on Honshu (Ishii 1999), and *S. miyosii* with “*S. sexspinosus*” (misidentified “*S. nipponicus*”) on Kyushu (Miyosi 1961). Both *S. elegans* and *S. miyosii* are unquestionably distinguishable from the sympatric species in that the cephalic marginal sulci are short (vs the sulci are complete, reaching anterior half of the cephalic plate in *S. rubiginosus*, *S. quadristriatus*, and “*S. nipponicus*”). One hypothesis for such a distributional pattern is that *S. elegans* and the three similar species arose through allopatric speciation events while they dispersed across the Far East Islands, long after they had diverged from the rest of the Asian/North American group. However, the phylogenetic analyses failed to resolve the relationships among *S. curtus* and the two new species. Additional phylogenetic studies are thus essential to reveal the biogeography and evolutionary history of these species.

Acknowledgments

The authors are grateful to Dr Gregory D. Edgecombe, and the two anonymous reviewers for their valuable comments and suggestions on this manuscript. We express our gratitude to Futaro Okuyama, Ryobu Fukuyama (Kyoto University; KU), Taiga Kato (KU), and Naoto Sawada (KU) for their help with collecting material. We also thank Dr Christopher Akcali (Edanz; <https://jp.edanz.com/ac>) for editing a draft of this manuscript. This study was supported by the Tokyo Metropolitan University Fund for TMU Strategic Research (Leader: Professor Noriaki Murakami at TMU; FY2020–FY2022) and the Sasakawa Scientific Research Grant from the Japan Science Society (Grant Number 2022-5017).

References

- Attems C. 1930. *Myriapoda 2. Scolopendromorpha*. Das Tierreich 54. De Gruyter, Berlin.
- Bonato L., Edgecombe G.D., Lewis J.G.E., Minelli A., Pereira L.A., Shelley R.M. & Zapparoli M. 2010. A common terminology for the external anatomy of centipedes (Chilopoda). *ZooKeys* 69: 17–51. <https://doi.org/10.3897/zookeys.69.737>
- Castresana J. 2000. Selection of conserved blocks from multiple alignments for their use in phylogenetic analysis. *Molecular Biology and Evolution* 17 (4): 540–552. <https://doi.org/10.1093/oxfordjournals.molbev.a026334>
- Chagas-Jr A. 2008. *Revisão Sistemática e Análise Filogenética dos Scolopocryptopinae (Chilopoda, Scolopendromorpha)*. PhD thesis, Universidade Federal do Rio de Janeiro, Rio de Janeiro, Brazil.
- Chagas-Jr A., Edgecombe G.D. & Minelli A. 2023. An unknown segment number in centipedes: a new species of *Scolopocryptops* (Chilopoda: Scolopendromorpha) from Trinidad with 25 leg-bearing segments. *Organisms Diversity & Evolution* 23: 369–380. <https://doi.org/10.1007/s13127-022-00591-7>
- Chao J.-L. & Chang H.-W. 2003. The scolopendromorph centipedes (Chilopoda) of Taiwan. *African Invertebrates* 44 (1): 1–11.
- Chao J.-L. & Chang H.-W. 2008. Neotype designation for two centipedes, *Scolopocryptops curtus* (Takakuwa, 1939) and *Cryptops nigropictus* Takakuwa, 1936, and a review of species of Scolopendromorpha (Chilopoda) in Taiwan. *Collection and Research* 21: 1–15.

- Demange J.M. & Richard J. 1969. Morphologie de l'appareil génital mâle des Scolopendromorphes et son importance en systématique (Myriapodes Chilopodes). *Bulletin du Muséum national d'histoire naturelle 2^e Série* 40 (5): 968–983.
- Edgecombe G.D. & Giribet G. 2004. Adding mitochondrial sequence data (16S rRNA and cytochrome *c* oxidase subunit I) to the phylogeny of centipedes (Myriapoda: Chilopoda): an analysis of morphology and four molecular loci. *Journal of Zoological Systematics and Evolutionary Research* 42 (2): 89–134. <https://doi.org/10.1111/j.1439-0469.2004.00245.x>
- Edgecombe G.D., Vahtera V., Stock S.R., Kallonen A., Xiao X., Rack A. & Giribet G. 2012. A scolopocryptopid centipede (Chilopoda: Scolopendromorpha) from Mexican amber: synchrotron microtomography and phylogenetic placement using a combined morphological and molecular data set. *Zoological Journal of the Linnean Society* 166 (4): 768–786. <https://doi.org/10.1111/j.1096-3642.2012.00860.x>
- Edgecombe G.D., Huey J.A., Humphreys W.F., Hillyer M., Burger M.A., Volschenk E.S. & Waldock J.M. 2019. Blind scolopendrid centipedes of the genus *Cormocephalus* from subterranean habitats in Western Australia (Myriapoda: Scolopendromorpha: Scolopendridae). *Invertebrate Systematics* 33 (6): 807–824. <https://doi.org/10.1071/IS19015>
- Folmer O., Black M., Hoeh W., Lutz R. & Vrijenhoek R. 1994. DNA primers for amplification of mitochondrial cytochrome *c* oxidase subunit I from diverse metazoan invertebrates. *Molecular Marine Biology and Biotechnology* 3 (5): 294–299.
- Garrick R.C., Newton K.E. & Worthington R.J. 2018. Cryptic diversity in the southern Appalachian Mountains: genetic data reveal that the red centipede, *Scolopocryptops sexspinosus*, is a species complex. *Journal of Insect Conservation* 22: 799–805. <https://doi.org/10.1007/s10841-018-0107-3>
- Hoang D.T., Chernomor O., Haeseler A., Minh B.Q. & Vinh L.S. 2017. UFBoot2: improving the Ultrafast Bootstrap approximation. *Molecular Biology and Evolution* 35 (2): 518–522. <https://doi.org/10.1093/molbev/msx281>
- Humbert A. & Saussure H. 1869. Myriapoda nova Americana. *Revue et Magasin de Zoologie pure et appliquée 2^e Série* 2 (21): 149–159. Available from <https://www.biodiversitylibrary.org/page/33749173> [accessed 17 Oct. 2023].
- Ikehara S. & Shimojana M. 1971. The terrestrial animals of Senkaku Islands. In: University of the Ryukyus Senkaku Islands Scientific Survey Team (ed.) *Senkaku Rettou Gakujutsu Chousa Houkoku [Senkaku Islands Scientific Survey Report]*: 85–114. University of the Ryukyus, Naha. [In Japanese with English abstract.]
- Iorio E. 2003. Morphologie externe des appareils génitaux mâle et femelle de la famille Scolopendridae (Chilopoda, Scolopendromorpha). *Bulletin de Phyllie* 16: 10–16.
- Ishii K. 1999. [A list and remarks on myriapod fauna in Chiba Prefecture]. In: The Biological Society of Chiba Prefecture (ed.) *Fauna of Chiba Prefecture*: 206–218. Bun-ichi Co., Ltd, Tokyo. [In Japanese.]
- Jonishi T. & Nakano T. 2022. Taxonomic accounts and phylogenetic positions of the Far East Asian centipedes *Scolopocryptops elegans* and *S. curtus* (Chilopoda: Scolopendromorpha). *Zoological Science* 39 (6): 581–593. <https://doi.org/10.2108/zs220029>
- Katoh K. & Standley D.M. 2013. MAFFT multiple sequence alignment software version 7: improvements in performance and usability. *Molecular Biology and Evolution* 30 (4): 772–780. <https://doi.org/10.1093/molbev/mst010>
- Katoh K., Rozewicki J. & Yamada K.D. 2019. MAFFT online service: multiple sequence alignment, interactive sequence choice and visualization. *Briefings in Bioinformatics* 20 (4): 1160–1166. <https://doi.org/10.1093/bib/bbx108>

- Koch L. 1878. Japanesische Arachniden und Myriapoden. *Verhandlungen der Kaiserlich-Königlichen Zoologisch-Botanischen Gesellschaft in Wien* 27: 735–798.
Available from <https://www.biodiversitylibrary.org/page/26709592> [accessed 17 Oct. 2023].
- Kumar S., Stecher G., Li M., Knyaz C. & Tamura K. 2018. MEGA X: Molecular Evolutionary Genetics Analysis across computing platforms. *Molecular Biology and Evolution* 35 (6): 1547–1549.
<https://doi.org/10.1093/molbev/msy096>
- Kuraku S., Zmasek C.M., Nishimura O. & Katoh K. 2013. aLeaves facilitates on-demand exploration of metazoan gene family trees on MAFFT sequence alignment server with enhanced interactivity. *Nucleic Acids Research* 41 (W1): W22–W28. <https://doi.org/10.1093/nar/gkt389>
- Lanfear R., Frandsen P.B., Wright A.M., Senfeld T. & Calcott B. 2016. PartitionFinder 2: new methods for selecting partitioned models of evolution for molecular and morphological phylogenetic analyses. *Molecular Biology and Evolution* 34 (3): 772–773. <https://doi.org/10.1093/molbev/msw260>
- Le S.X., Schileyko A.A. & Nguyen A.D. 2023. A review of Vietnamese *Scolopocryptops* Newport, 1844 (Chilopoda: Scolopendromorpha), with a description of *S. hoanglieni* n. sp. and the updated generic list of species. *Zootaxa* 5228 (4): 411–447. <https://doi.org/10.11646/zootaxa.5228.4.3>
- Lewis J.G.E., Edgecombe G.D. & Shelley R.M. 2005. A proposed standardised terminology for the external taxonomic characters of the Scolopendromorpha (Chilopoda). *Fragmenta Faunistica* 48 (1): 1–8.
- Linnaeus C. 1767. *Systema naturæ per regna tria naturæ, secundum classes, ordines, genera, species, cum characteribus, differentiis, synonymis, locis. Tom. I. Pars II. Editio duodecima, reformata.* Laurentius Salvius, Stockholm [Holmiae].
- McNeil J. 1887. Description of twelve new species of Myriapoda, chiefly from Indiana. *Proceedings of the United States National Museum* 10 (632): 328–334. <https://doi.org/10.5479/si.00963801.10-632.328>
- Miyosi Y. 1961. *Otocryptops curtus* found in Kyûshû. *Collecting and Breeding* 23 (6): 180–181. [In Japanese.]
- Miyosi Y. 1971. *Otocryptops curtus* Takakuwa. In: Okada K., Uchida S. & Uchida T. (eds) *New Illustrated Encyclopedia of the Fauna of Japan, 3rd Ed.*: 734. Hokuryûkan, Tokyo. [In Japanese.]
- Murienne J., Edgecombe G.D. & Giribet G. 2011. Comparative phylogeography of the centipedes *Cryptops pictus* and *C. niuensis* (Chilopoda) in New Caledonia, Fiji and Vanuatu. *Organisms Diversity & Evolution* 11 (1): 61–74. <https://doi.org/10.1007/s13127-011-0041-7>
- Newport G. 1844. Monograph of the class Myriapoda, order Chilopoda; with observations on the general arrangement of the Articulata. Part I. *Transactions of the Linnean Society of London* 19 (3): 265–302.
<https://doi.org/10.1111/j.1096-3642.1842.tb00368.x>
- Nguyen L.T., Schmidt H.A., von Haeseler A. & Minh B.Q. 2015. IQ-TREE: a fast and effective stochastic algorithm for estimating maximum-likelihood phylogenies. *Molecular Biology and Evolution* 32 (1): 268–274. <https://doi.org/10.1093/molbev/msu300>
- Ogawa K. 1961. Chromosome studies in the Myriapoda, XVI. The chromosomes of five species of chilopods. *Zoological Magazine* 70 (7): 203–206. [In Japanese with English abstract.]
<https://www.doi.org/10.34435/zm003988>
- Ômine T. 1969. On the chilopods collected from the Ryukyu Islands. *Okidai Ronso* 9 (1): 269–298. [In Japanese.]

- Ômine T. 1987. [Chilopods of Kunigami district]. In: Okinawa Prefectural Board of Education (ed.) *Special Animals of Kunigami District in Okinawa Island*: 37–39. Okinawa Prefectural Board of Education, Naha. [In Japanese.]
- Ômine T. 2002. [Characteristics of the distribution of myriapods in the Ryukyu Archipelago]. In: Kimura M. (ed.) [*Formation and Introduction of Organisms of the Ryukyu Archipelago*]: 151–162. Okinawa Times, Naha. [In Japanese.]
- Ômine T. & Itô Y. 1998. Abundance and diversity of soil macrofauna of forests in Yanbaru, northern montane part of Okinawa Island, with special reference to removal of undergrowth. *Okinawa Daigaku Kiyô* 15: 131–159.
- Peretti E., Cecchin C., Fusco G., Gregnanin L., Kos I. & Bonato L. 2022. Shedding light on species boundaries in small endogeic animals through an integrative approach: species delimitation in the centipede *Clinopodes carinthiacus* (Chilopoda: Geophilidae) in the south-eastern Alps. *Zoological Journal of the Linnean Society* 196 (2): 902–923. <https://doi.org/10.1093/zoolinlean/zlac008>
- Pocock R.I. 1890. A short account of a small collection of Myriopoda obtained by Mr. Edward Whymper in the Andes of Ecuador. *Annals and Magazine of Natural History, Series 6* 6 (32): 141–146. <https://doi.org/10.1080/00222939008694014>
- Pocock R.I. 1895. Chilopoda. Part CXXVI. In: Godman F.D. & Salvin O. (eds) *Biologia Centrali-Americana. Volume 14. Chilopoda and Diplopoda*: 1–24. Taylor & Francis, London. <https://doi.org/10.5962/bhl.title.730>
- Pocock R.I. 1896. Chilopoda. Part. CXXVI. In: Godman F.D. & Salvin O. (eds) *Biologia Centrali-Americana. Volume 14. Chilopoda and Diplopoda*: 25–40. Taylor & Francis, London. <https://doi.org/10.5962/bhl.title.730>
- Puillandre N., Lambert A., Brouillet S. & Achaz G. 2011. ABGD, Automatic Barcode Gap Discovery for primary species delimitation. *Molecular Ecology* 21: 1864–1877. <https://doi.org/10.1111/j.1365-294X.2011.05239.x>
- Puillandre N., Brouillet S. & Achaz G. 2021. ASAP: assemble species by automatic partitioning. *Molecular Ecology Resources* 21: 609–620. <https://doi.org/10.1111/1755-0998.13281>
- Rambaut A., Drummond A.J., Xie D., Baele G. & Suchard M.A. 2018. Posterior summarization in Bayesian phylogenetics using Tracer 1.7. *Systematic Biology* 67 (5): 901–904. <https://doi.org/10.1093/sysbio/syy032>
- Ronquist F., Teslenko M., van der Mark P., Ayres D.L., Darling A., Höhna S., Larget B., Liu L., Suchard M.A. & Huelsenbeck J.P. 2012. MrBayes 3.2: efficient Bayesian phylogenetic inference and model choice across a large model space. *Systematic Biology* 61 (3): 539–542. <https://doi.org/10.1093/sysbio/sys029>
- Say T. 1821. Descriptions of the Myriapodæ of the United States. *Journal of the Academy of Natural Sciences of Philadelphia* 2 (1): 102–114. Available from <https://www.biodiversitylibrary.org/page/36831290> [accessed 17 Oct. 2023].
- Schileyko A.A. 2014. A contribution to the centipede fauna of Venezuela (Chilopoda: Scolopendromorpha). *Zootaxa* 3821 (1): 151–192. <https://doi.org/10.11646/zootaxa.3821.2.1>
- Schileyko A.A. 2018. A contribution to the knowledge of the centipedes of Saint Barthélemy Island (French Antilles), with re-descriptions of *Newportia heteropoda* Chamberlin, 1918 and *Cormocephalus impressus* Porat, 1876 (Chilopoda: Scolopendromorpha). *Zootaxa* 4438 (1): 59–78. <https://doi.org/10.11646/zootaxa.4438.1.2>

- Schwendinger P.J. & Giribet G. 2005. The systematics of the south-east Asian genus *Fangensis* Rambla (Opiliones: Cyphophthalmi: Stylocellidae). *Invertebrate Systematics* 19 (4): 297–323. <https://doi.org/10.1071/IS05023>
- Shelley R.M. 2002. *A Synopsis of the North American Centipedes of the Order Scolopendromorpha (Chilopoda)*. Virginia Museum of Natural History Memoir 5, Virginia Museum of Natural History, Virginia.
- Shinohara K. 1949. Notes on centipedes collected by Mr. Fujiyama in Hachijo Island. *Acta Arachnologica* 11 (3–4): 80–85. [In Japanese.] <https://doi.org/10.2476/asjaa.11.80>
- Shinohara K. 1984. Two new species of the *Scolopocryptops* from Japan (Chilopoda: Cryptopidae). *Edaphologia* 31: 39–42.
- Shinohara K. 1990. A new species of the genus *Scolopocryptops* (Chilopoda: Cryptopidae) from Japan. *Proceedings of the Japanese Society of Systematic Zoology* 41: 62–65. https://doi.org/10.19004/pjssz.41.0_62
- Takakuwa Y. 1933. [Miscellaneous notes on centipedes. IX. (External morphology of *Otocryptops*)]. *Hakubutsugaku Zasshi* 31 (49): 11–22. [In Japanese.]
- Takakuwa Y. 1937. Eine neue Art von *Otocryptops* und ihre geographische Verbreitung in Japan. *Dobutsugaku Zasshi* 49 (6): 203–205. [In Japanese with German abstract and description.] <https://www.doi.org/10.34435/zm002540>
- Takakuwa Y. 1939. A new species of genus *Otocryptops* from Japan. *Dobutsugaku Zasshi* 51 (10): 698–700. [In Japanese with German description.]
- Takakuwa Y. 1940. *Scolopendromorpha (Class Chilopoda: Epimorpha)*. Fauna Nipponica, Vol. IX, Fasc. VIII, No. II, Sanseido, Tokyo. [In Japanese.]
- Takano M. 1979. [Littoral myriapods in Niijima Island Miyakejima Island, Izu Islands]. *Takakuwaia* 11: 5–7. [In Japanese.]
- Takashima H. 1949. The general view of Japanese myriapods. *Acta Arachnologica* 11 (1–2): 8–25. [In Japanese.] <https://doi.org/10.2476/asjaa.11.8>
- Vahtera V., Edgecombe G.D. & Giribet G. 2012. Evolution of blindness in scolopendromorph centipedes (Chilopoda, Scolopendromorpha): insight from an expanded sampling of molecular data. *Cladistics* 28 (1): 4–20. <https://doi.org/10.1111/j.1096-0031.2011.00361.x>
- Vahtera V., Edgecombe G.D. & Giribet G. 2013. Phylogenetics of scolopendromorph centipedes: can denser taxon sampling improve an artificial classification? *Invertebrate Systematics* 27 (5): 578–602. <https://doi.org/10.1071/IS13035>
- Verhoeff K.W. 1934. Beiträge zur Systematik und Geographie der Chilopoden. *Zoologische Jahrbücher Abteilung für Systematik, Ökologie und Geographie der Tiere* 66 (1–2): 1–112.
- Whiting M.F., Carpenter J.M., Wheeler Q.D. & Wheeler W.C. 1997. The Strepsiptera problem: phylogeny of the holometabolous insect orders inferred from 18S and 28S ribosomal DNA sequences and morphology. *Systematic Biology* 46 (1): 1–68. <https://doi.org/10.1093/sysbio/46.1.1>
- Wood Jr. H.C. 1862. On the Chilopoda of North America, with a catalogue of all the specimens in the collection of the Smithsonian Institution. *Journal of the Academy of Natural Sciences of Philadelphia, Second Series* 5 (1): 5–52. <https://doi.org/10.5962/bhl.title.1585>

Manuscript received: 19 December 2022

Manuscript accepted: 6 July 2023

Published on: 24 November 2023

Topic editor: Tony Robillard

Secton editor: Nesrine Akkari

Desk editor: Pepe Fernández

Printed versions of all papers are also deposited in the libraries of the institutes that are members of the *EJT* consortium: Muséum national d’histoire naturelle, Paris, France; Meise Botanic Garden, Belgium; Royal Museum for Central Africa, Tervuren, Belgium; Royal Belgian Institute of Natural Sciences, Brussels, Belgium; Natural History Museum of Denmark, Copenhagen, Denmark; Naturalis Biodiversity Center, Leiden, the Netherlands; Museo Nacional de Ciencias Naturales-CSIC, Madrid, Spain; Leibniz Institute for the Analysis of Biodiversity Change, Bonn – Hamburg, Germany; National Museum of the Czech Republic, Prague, Czech Republic.